International Journal of Precision Engineering and Manufacturing
https://doi.org/10.1007/s12541-025-01229-2

Online ISSN 2005-4602
Print ISSN 2234-7593

REGULAR PAPER

Prediction of Dimensional Accuracy and Surface Quality in Additively Manufactured Biomedical Implants Using ANN

Arif Karadag[1] · **Osman Ulkir**[2]

Received: 25 December 2024 / Revised: 24 January 2025 / Accepted: 30 January 2025

Abstract

This study investigates the prediction of fused deposition modeling (FDM) process parameters for manufacturing biomedical implants with high dimensional accuracy and surface quality. Biomedical implants were fabricated in circular, triangular, and pentagonal geometries to accommodate different anatomical requirements, using three materials selected for their biomedical applicability and mechanical properties. These materials are polylactic acid (PLA), polyethylene terephthalate glycol, and thermoplastic polyurethane (TPU). This research utilizes the Taguchi L27 orthogonal array methodology to analyze the influence of five critical printing parameters: material type, layer thickness (200–300–400 µm), infill density (30%–60%–90%), infill pattern (zigzag, cubic, and triangle), and wall thickness (1–2–3 mm). The analysis of variance demonstrated that material type and layer thickness are the most significant factors, contributing 49.25% and 17.97%, respectively, to dimensional accuracy in circular geometries. Surface roughness measurements showed that layer thickness (30.95%) and material type (31.28%) are dominant factors affecting surface quality. The optimum parameters for dimensional accuracy were determined as PLA material, zigzag infill pattern, 2 mm wall thickness, 30% infill density and 200 µm layer thickness, while the highest surface quality was achieved with PLA material, triangle infill pattern, 3 mm wall thickness, 90% infill density and 200 µm layer thickness. An artificial neural network model was developed to predict dimensional accuracy and surface quality, achieving high correlation coefficients ($R^2 > 0.96$) between predicted and experimental results across all geometric configurations. These findings offer valuable guidelines for predicting and optimizing parameters in FDM-based biomedical implant manufacturing, advancing precision medicine by enhancing additive manufacturing processes and implant performance.

Keywords Additive manufacturing · Biomedical implant · Surface roughness · Artificial neural network · Dimensional accuracy

1 Introduction

Additive manufacturing (AM) has revolutionized biomedical implant fabrication, fundamentally transforming the approach to medical device design and production [1, 2]. The ability of AM to create intricate designs with remarkable accuracy and customizable features has transformed the field of advanced implants and prosthetics [3–5]. Traditional manufacturing methods often encounter significant limitations, including restricted design flexibility, substantial material wastage, high production costs, and lengthy manufacturing cycles [6]. In contrast, AM, particularly fused deposition modeling (FDM), effectively addresses these challenges [7, 8]. FDM provides unique benefits, including greater design freedom, the capability to create highly intricate structures that are unattainable with conventional methods, and the flexibility to customize designs for patient-specific requirements [9–11]. Moreover, its rapid prototyping capabilities significantly reduce development time, allowing for faster iterations and improvements in design. These features make FDM an indispensable tool in precision medicine, supporting the creation of implants that not only fit individual anatomical structures but also integrate seamlessly into the body [12, 13]. Furthermore, the technology's cost-effectiveness and adaptability to a wide range of

✉ Osman Ulkir
o.ulkir@alparslan.edu.tr

Arif Karadag
a.karadag@alparslan.edu.tr

[1] Department of Motor Vehicles and Transportation Technologies, Mus Alparslan University, 49250 Mus, Turkey

[2] Department of Electric and Energy, Mus Alparslan University, 49250 Mus, Turkey

Published online: 12 February 2025

biocompatible materials underscore its value in advancing biomedical applications, paving the way for more accessible, efficient, and personalized healthcare solutions.

Dimensional accuracy and surface quality are vital factors in biomedical implant fabrication, as they have a direct impact on implant performance and patient outcomes [14, 15]. The success of an implant depends on multiple factors, including geometric precision, surface characteristics, and material properties. Surface roughness particularly affects tissue integration, bacterial adhesion, and overall biocompatibility, while dimensional accuracy ensures proper fit and functionality within anatomical structures [16]. Excessive surface roughness can result in adverse tissue reactions and implant rejection, while dimensional inaccuracies may lead to mechanical instability or tissue damage [17]. The selection of materials plays a vital role in determining both dimensional accuracy and surface quality [18–20]. This study investigates three widely used materials in biomedical applications: polylactic acid (PLA), polyethylene terephthalate glycol (PETG), and thermoplastic polyurethane (TPU). Each material offers unique advantages: PLA provides excellent biocompatibility and biodegradability [12], PETG ensures dimensional stability [21], and TPU contributes flexibility and durability [22]. The prediction and optimization of processing parameters for each material is crucial, as their behavior varies significantly during the FDM process [23–26].

The prediction of FDM parameters represents a complex challenge in achieving the desired balance between mechanical integrity and biocompatibility. Key parameters including layer thickness, infill density, infill pattern, and wall thickness significantly influence both surface quality and dimensional accuracy [27–29]. The Taguchi method offers a robust statistical approach for prediction and optimization of these parameters, enabling systematic evaluation of their effects on implant quality. This method has proven particularly effective in minimizing surface roughness and enhancing geometric accuracy in FDM-produced implants.

There are limited studies in the literature on the dimensional accuracy and surface quality of biomedical products produced using the FDM [30–33]. Sai et al. investigated the impact of FDM process parameters—layer thickness, raster angle, infill density, and internal structure—on the surface roughness, build time, and compressive strength of biomedical implants [34]. Experimental data were modeled using an adaptive neuro-fuzzy inference system (ANFIS) within a face-centered central composite design framework to predict outcomes. Results showed that the ANFIS approach accurately identifies optimal FDM parameter combinations, balancing quality and efficiency. Balasubramanian et al. explored the optimization of FDM process parameters to minimize circularity error and surface roughness in the fabrication of biomedical implants [35]. The study examined the effects of printing temperature, speed, and layer thickness. Results indicated that build orientation significantly influenced circularity error, while layer thickness had the greatest impact on roughness. Optimized parameters reduced circularity error by 42% and Ra by 67% compared to default settings. Sakthivel et al. investigated the optimization of FDM parameters for fabricating PLA–stainless-steel composite biomedical implants [36]. This novel composite material combines the biocompatibility of PLA and stainless steel, addressing the mechanical limitations of pure polymer components. The research optimized FDM parameters using a design of experiments approach and demonstrated the composite's functional properties through tensile and impact tests. Biocompatibility tests with pre-osteoblast cells confirmed the composite retained PLA's biocompatibility. The results highlight the potential of low-cost FDM printers for producing next-generation biomaterials with tailored properties for biomedical implants. Gregory et al. examined the use of FDM in producing biomedical devices such as bone and tooth implants, tissue repair patches, nerve guidance conduits (NGCs), and coronary artery stents [37]. The study proposed CAD designs and fabricated proof-of-concept prototypes using a cost-effective 3D printer, highlighting design and slicing challenges and suggesting optimizations for complex biomedical applications. Patient-specific implants were generated from CT scans using mirroring and mesh mixing techniques. A PLA/PHA filament blend was characterized, showing tensile properties suitable for stents, NGCs, and bone scaffolds. The research also demonstrated FDM's potential for soft tissue applications, recommending more elastomeric MCL-PHAs for enhanced performance.

Recent advances in artificial intelligence, particularly artificial neural networks (ANNs), have opened new possibilities for predicting and optimizing FDM processes [38–40]. Traditional methods often struggle with the complex, nonlinear relationships between printing parameters and final part quality. ANNs excel at capturing these intricate relationships, enabling more accurate predictions of dimensional accuracy and surface quality [41, 42]. This predictive capability is particularly valuable in biomedical applications, where consistent quality and reliability are paramount. Previous studies have primarily focused on predicting individual aspects of the FDM process or specific geometric shapes. However, there remains a critical gap in understanding how multiple process parameters simultaneously affect both dimensional accuracy and surface quality across different geometric shapes and materials relevant to biomedical applications.

This study addresses these limitations by comprehensively investigating the optimization of FDM process parameters for biomedical implant fabrication. The Taguchi L27 orthogonal array methodology is employed to investigate four crucial printing parameters: layer thickness, infill

density, infill pattern, and wall thickness. The study's novelty lies in its integrated approach to analyzing both dimensional accuracy and surface quality across multiple materials (PLA, PETG, and TPU) and geometries (circular, triangle, and pentagon), supported by ANN-based prediction models. Specifically, this research aims to: (1) determine optimal printing parameters for achieving high dimensional accuracy and surface quality in biomedical implants, (2) evaluate the effectiveness of ANN models in predicting FDM process outcomes, with validation through experimental results showing R^2 values exceeding 96%, and (3) establish comprehensive guidelines for material-specific parameter optimization in biomedical implant fabrication. The findings will contribute significantly to advancing the reliability and efficiency of FDM-based biomedical implant manufacturing.

2 Materials and Methods

2.1 3D Printing Process

The biomedical implant was fabricated using the FDM method on a Creality K1C 3D printer. The implant design, which incorporated basic geometries such as circular, triangular, and pentagonal shapes to meet the functional and structural requirements of biomedical applications, was developed in SolidWorks software. The technical drawing and 3D image of the model, which illustrate these geometries, are shown in Fig. 1. Following the design phase, the model was exported in standard triangle language (STL) format and converted into G-code using slicing software (Creality Print), ensuring accurate instructions for the FDM printing process.

The FDM process begins with the heating of the printer's nozzle, which in the case of the Creality K1C can reach temperatures up to 300 °C, enabling the use of various thermoplastic materials. During the process, the filament is fed through a dual-gear extruder system to ensure consistent material flow. The filament, such as PLA, PETG, or TPU, is melted as it passes through the heated nozzle and is deposited layer by layer onto the build platform. The build platform itself is heated to enhance adhesion and reduce warping, creating a stable foundation for the printed layers [43–45]. As the layers are deposited, they cool and solidify, gradually forming the desired geometry of the implant.

PLA, PETG, and TPU materials were chosen for their unique properties and suitability for biomedical applications. PLA, being biodegradable and biocompatible, is often used for temporary implants and scaffolds in tissue engineering [46]. PETG offers a balance between durability and chemical resistance, making it ideal for drug delivery devices and robust implant components [47]. TPU, with its exceptional elasticity and flexibility, is suited for applications requiring soft and adaptable materials, such as wearable biomedical devices [48]. The specific properties of these materials, including their mechanical and thermal characteristics, are shown in Table 1. The Creality K1C printer enhanced the efficiency and precision of the manufacturing process

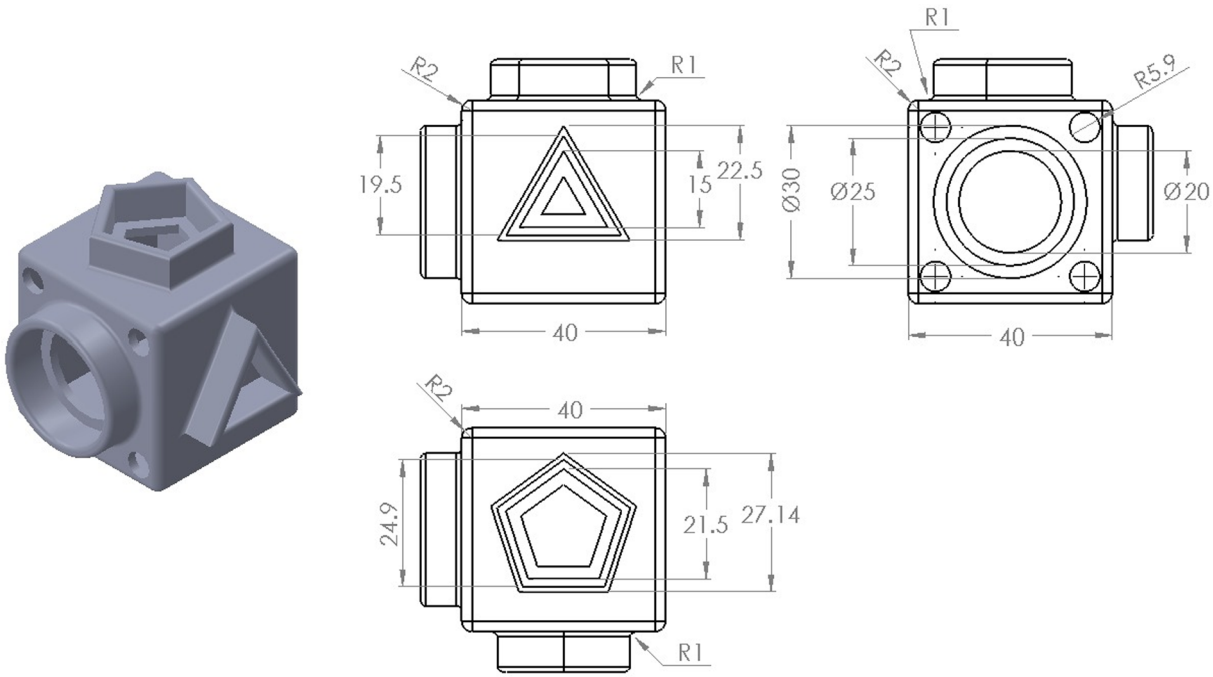

Fig. 1 Technical drawing and 3D model of the designed biomedical implant sample

Table 1 The description of the PLA, PETG, and TPU printing materials

Properties	Description		
	PLA	PETG	TPU
Color	Yellow	Blue	Green
Wire diameter	1.75 ± 0.05 mm	1.75 ± 0.05 mm	1.75 ± 0.05 mm
Recommended printing temperature	190–220 °C	230–260 °C	190–240 °C
Recommended printing speed	40–120 mm/s	25–75 mm/s	20–50 mm/s
Bed platform temperature	60–80 °C	60–100 °C	60–90 °C
Filament density	1.24 g/cm^3	1.27 g/cm^3	1.21 g/cm^3

through features such as automatic bed leveling, an enclosed design for stable thermal conditions, and high-speed printing capabilities of up to 600 mm/s. Its build volume of 220 × 220 × 250 mm provided flexibility for creating both intricate small components and larger prototypes. This integration of advanced material properties, optimized process parameters, and precise control in the FDM process highlights its ability to meet the demanding requirements of biomedical applications, paving the way for customized and high-quality implant production.

2.2 Design of Experiment

In this study, the experimental design process aimed at investigating the relationship between 3D printing parameters and two key quality metrics—surface roughness and dimensional accuracy—during the fabrication of biomedical implants. The Taguchi method was employed as it is a robust statistical tool that enables the optimization of processes by systematically evaluating the effects of various parameters with a minimal number of experiments [49, 50]. This method not only minimizes cost and time but also provides comprehensive insights into the interaction of process parameters, allowing for the identification of optimal conditions. Its graphical analysis capabilities further aid in visualizing the influence of parameters and their levels on process performance. When compared to other experimental design techniques, Taguchi stands out for its ability to analyze the effects of more parameters while minimizing the number of trials required. For example, the Box-Behnken design method offers the ability to examine a wider combination of factors, but this requires more experimental data [51]. This makes the Taguchi method a more practical and cost-effective alternative. On the other hand, one of the most obvious weaknesses of Taguchi is that it can ignore some complex interactions. For example, in systems that require more comprehensive and detailed interaction analysis, methodologies that consider the interactions of factors, such as the full factorial design, may be more appropriate. As a result, the Taguchi is suitable for resource-constrained projects that require systematic and rapid results, while it may be limited compared to other methods in cases where complex interactions and more detailed data analysis are required.

The fabrication of biomedical implants required careful control of five key printing parameters to ensure reliability: material type, layer thickness (LT), infill density (ID), infill pattern (IP), and wall thickness (WT). These parameters are shown in Table 2. The selection of these parameters was based on their significant influence on both surface quality and dimensional accuracy, as highlighted in the literature. The material type (PLA, PETG, and TPU) was chosen due to the distinct properties of these materials in biomedical applications. The inclusion of these materials allows for an in-depth evaluation of their effects on both surface roughness and dimensional accuracy. LT is a critical parameter that affects the resolution and surface finish of printed parts. Thinner layers generally result in smoother surfaces and higher precision, contributing to both better surface roughness and dimensional accuracy. However, thicker layers reduce printing time, highlighting the need to balance these factors for optimized results. ID was included because it significantly impacts both the mechanical properties and dimensional stability of the printed parts. While lower infill densities reduce weight and material usage, higher densities increase structural integrity, which is crucial for maintaining dimensional accuracy in biomedical implants. IP, including zigzag, cubic, and triangular patterns, influences not only the internal structure and mechanical performance but also the surface uniformity and dimensional consistency of the parts. The study examines the individual characteristics that make each pattern unique. WT was selected because of its role in determining the strength, stability, and dimensional

Table 2 The experimental design parameters and levels of the Taguchi

Factors	Level 1	Level 2	Level 3
Material	PLA	PETG	TPU
Layer thickness (LT), μm	200	300	400
Infill density (ID), %	30	60	90
Infill pattern (IP)	Zigzag	Cubic	Triangle
Wall thickness (WT), mm	1	2	3

reliability of the printed parts. Thicker walls provide greater mechanical support, while thinner walls enhance flexibility, making this parameter critical for balancing strength and dimensional precision.

This study systematically examines these parameters and their levels using the Taguchi method to understand their combined and individual effects on surface roughness and dimensional accuracy. The optimization of these factors is intended to elevate the quality and performance of FDM-produced biomedical implants, aligning them with the stringent requirements of modern medical applications. The experimental design process was carried out using Taguchi L27 orthogonal array to determine the optimum values of FDM parameters and to minimize cost and time by reducing the number of experiments. This array provided by the Taguchi method provided a more efficient experimental process by reducing the number of experiments from 243 to 27. Each experiment was repeated three times and reliable results were obtained to obtain optimum surface roughness and dimensional accuracy. The dimensional accuracy of each geometric part was evaluated by measuring its diameter and its x and y planes. Measurements were made from a single surface to determine surface roughness. The stability of the parameters and minimum process variability were ensured by using the signal-to-noise (S/N) ratio. This ratio is a metric representing the ratio of the desired signal to the unwanted noise in a process. In quality improvement studies such as the Taguchi method, the S/N ratio is used to evaluate the stability, precision and performance of the process. A high S/N ratio indicates better performance with less variation. The experimental design performed according to the Taguchi method is given in Table 3. Measurements of dimensional accuracy and surface roughness were carried out as part of these experiments. Only the average surface roughness results are shown in this table. Dimensional accuracy results are given in the next section.

Table 3 Measured responses: results for surface roughness of ABS, PLA, and PETG samples

No	Process parameter					Experimental results
	Material	Layer thickness	Infill density	Infill pattern	Wall Thickness	Surface roughness (Ra_Mean (μm))
1	PLA	200	30	Zigzag	1	14.75
2	PLA	200	30	Zigzag	2	13.59
3	**PLA**	**200**	**30**	**Zigzag**	**3**	**12.32**
4	PLA	300	60	Cubic	1	15.78
5	PLA	300	60	Cubic	2	14.35
6	PLA	300	60	Cubic	3	13.16
7	PLA	400	90	Triangles	1	17.43
8	PLA	400	90	Triangles	2	15.63
9	PLA	400	90	Triangles	3	13.85
1	PETG	200	60	Triangles	1	18.01
2	PETG	200	60	Triangles	2	16.59
3	PETG	200	60	Triangles	3	14.98
4	PETG	300	90	Zigzag	1	22.56
5	PETG	300	90	Zigzag	2	20.58
6	PETG	300	90	Zigzag	3	18.95
7	PETG	400	30	Cubic	1	35.74
8	PETG	400	30	Cubic	2	32.71
9	PETG	400	30	Cubic	3	30.05
1	TPU	200	90	Cubic	1	20.48
2	TPU	200	90	Cubic	2	18.91
3	TPU	200	90	Cubic	3	17.05
4	TPU	300	30	Triangles	1	26.25
5	TPU	300	30	Triangles	2	23.98
6	TPU	300	30	Triangles	3	21.95
7	TPU	400	60	Zigzag	1	38.25
8	TPU	400	60	Zigzag	2	35.12
9	TPU	400	60	Zigzag	3	31.95

The bold text indicates the experiment in which the lowest surface roughness value was measured

2.3 Experimental Procedure

In this study, the effect of printing parameters on the dimensional accuracy and surface quality of the biomedical implant model produced by the FDM was investigated. This model has three different geometric shapes (Fig. 1). Circular, triangle (15.14 mm × 22.5 mm), and pentagon (26.45 mm × 27.14 mm) parts were used in the model. The reason for choosing these shapes is to ensure compatibility with the requirements of various biomedical implants such as tissue engineering or drug delivery devices. The FDM process was performed in accordance with the experiments in Table 3 determined by the Taguchi. Each sample was fabricated three times and a total of 81 parts were prepared for the test. 27 samples fabricated from PLA, PETG and TPU materials are shown in Fig. 2.

Surface roughness is a critical parameter that determines the overall quality of manufactured parts and is particularly important in biomedical implant production. Surface roughness directly affects the interaction, performance and biocompatibility of implants with tissue in biomedical applications. Surface irregularities and microscopic deviations are key factors affecting the implant's integration with tissues and its performance in the body. Therefore, surface roughness measurements play a vital role in ensuring the safety and effectiveness of implants. In this study, the surface quality of biomedical implants manufactured using FDM was evaluated in detail. Surface roughness measurements were performed using the Mitutoyo Surftest SJ-210 digital profilometer. The profilometer works by touching surface profiles with micron-level precision. Before the measurement, the necessary calibration procedures were performed so that the device could provide accurate results. During the measurement, the probe of the device was carefully moved along the specified surface of the part and micron-level height changes on the surface were detected. The obtained data was converted into a data set to determine the roughness properties of the surface, and the average surface roughness value (Ra) was automatically calculated by the device. The Ra value is a parameter that quantitatively expresses the surface roughness and is measured in microns (μm). A lower Ra value represents a smoother surface, while a higher Ra value indicates a rougher surface. The surface roughness of each part was measured three times to ensure accuracy, and the averages of the results were used. Figure 3 displays one of the surfaces analyzed in the study. The average Ra values regarding the results of the measurements are given in Table 3. This comprehensive evaluation is extremely important in understanding the surface roughness properties of biomedical implants fabricated with the FDM and determining the effects of production parameters on surface quality.

Dimensional accuracy is a critical factor in biomedical implant production that directly affects both functional performance and biological compatibility. Achieving the geometric dimensions established during the design phase

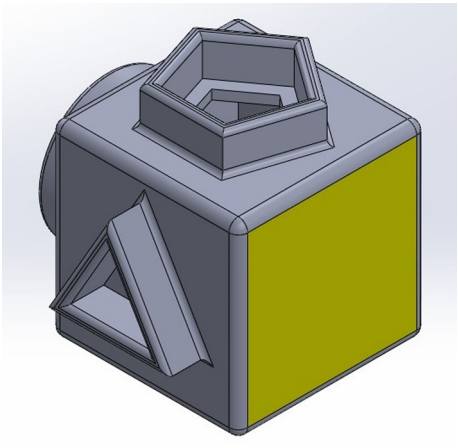

Fig. 3 Surface roughness measured in one area

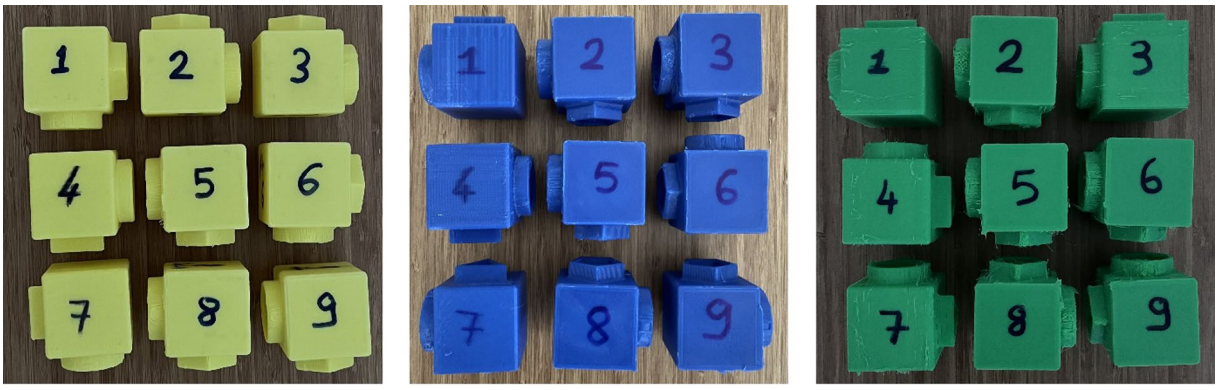

Fig. 2 The fabricated PLA, PLA and PETG test samples via fused deposition modeling

ensures proper anatomical fit and correct positioning of implants. Precision is particularly crucial for seamless tissue integration, adequate mechanical durability, and long-term functional effectiveness. Any dimensional deviations can adversely affect the implant's integration with biological tissues or its efficacy in surgical procedures. This study examined the dimensional accuracy of biomedical implant models manufactured using FDM. Three samples were produced for each of three different geometric shapes and measured using a precision digital caliper. Critical dimensions of each sample were evaluated, and the means and standard deviations of the measured values were calculated. This analysis provides valuable data for understanding the effects of manufacturing parameters on dimensional accuracy and implementing necessary process improvements. The measurement results were used to evaluate the accuracy of implant designs and the reliability of the manufacturing process.

3 Results and Discussion

3.1 Evaluation of the Measurement Results

This section presents the analysis of dimensional accuracy measurements obtained from biomedical implant components produced through FDM manufacturing. Dimensional accuracy refers to the conformity of the geometric dimensions determined in the design phase in the part obtained after production and is a critical parameter for biomedical implants. The dimensional accuracy of the parts produced with the FDM was carefully analyzed to understand whether the implants meet the design requirements. In addition to assessing dimensional accuracy, the study included material consumption and printing time as part of the evaluation criteria for the production process. These two parameters are important elements that affect the production cost, energy consumption and time management in FDM. Material consumption and printing time data were determined using 'Creality Print,' the slicing program associated with the 3D printer used in this study. The slicing program allows the model to be separated into layers and estimates the amount of filament needed during printing, the printing time and other printing parameters. While material consumption is important in terms of preventing waste in the production process and minimizing costs, printing time directly affects the efficiency of the production line. Efficient and budget-friendly production processes, especially in the field of biomedicine, provide considerable advantages. Consequently, the study evaluated not only dimensional accuracy but also the economic and time efficiency of the printing process.

When the comparative analysis of the printing times and material consumption of 3D printer materials (PLA, PETG and TPU) was made, the unique characteristics of each material were observed (Fig. 4). In PLA tests, printing times varied between 62–82 min, while material consumption was in the range of 35.5–41 gr (Fig. 4a). The highest material consumption was measured as 41 gr in experiment number 7, while the lowest consumption was recorded as 35.5 gr in experiment number 1. In PETG samples, printing times were between 55–95 min, and material consumption was in the range of 33–40 gr, with experiment number 4 showing the highest material consumption (40 gr) and experiment number 7 showing the lowest consumption (33 gr) (Fig. 4b). In TPU, low printing speeds were used due to its flexible structure, therefore printing times were in a very wide range of 80–220 min (Fig. 4c). While the material consumption of TPU varied between 29–35 gr, experiment number 1 exhibited the highest material consumption (35 gr), and experiment number 6 exhibited the lowest consumption (30 gr). These results show that the optimum printing parameters of each material are different and that flexible materials such as TPU require special attention during the printing process. The relationship between printing time and material consumption varies according to the material type, and this is an important factor to be considered in the optimization of 3D printing processes.

In this study, biomedical implant models with different geometric structures (circular, triangular and pentagonal) were developed (Fig. 1). Diversification of the geometric structures of biomedical implants is of critical importance in terms of adapting to different anatomical regions. As an example, circular designs are commonly applied in long bones, while triangular and pentagonal configurations may be more appropriate for joints or irregular bone structures. Therefore, geometric diversity in implant design provides a significant advantage in personalized medical applications. Dimensional accuracy is of great importance in implants produced with FDM. The exact fit of the implant to the patient's anatomy is critical for surgical success and patient comfort. In addition, dimensional deviations can directly affect the mechanical properties and load-bearing capacity of the implant. Therefore, the diameters of sections with circular geometry were measured during the study, while the dimensions of the triangular and pentagonal parts in the x–y direction were precisely recorded.

Three samples were fabricated from each sample and standard deviation values were calculated to increase the reliability of the measurements. Low standard deviation values (maximum 0.05) indicate that the production process is consistent and repeatable. These values are also used as an important indicator in the quality control of the production process. Low standard deviation indicates that implants will provide consistent results in clinical use, which is critical for patient safety. Table 4 shows the average diameter and standard deviation values of the circular part produced with a diameter of 30 mm, and Tables 5 and 6 show the average

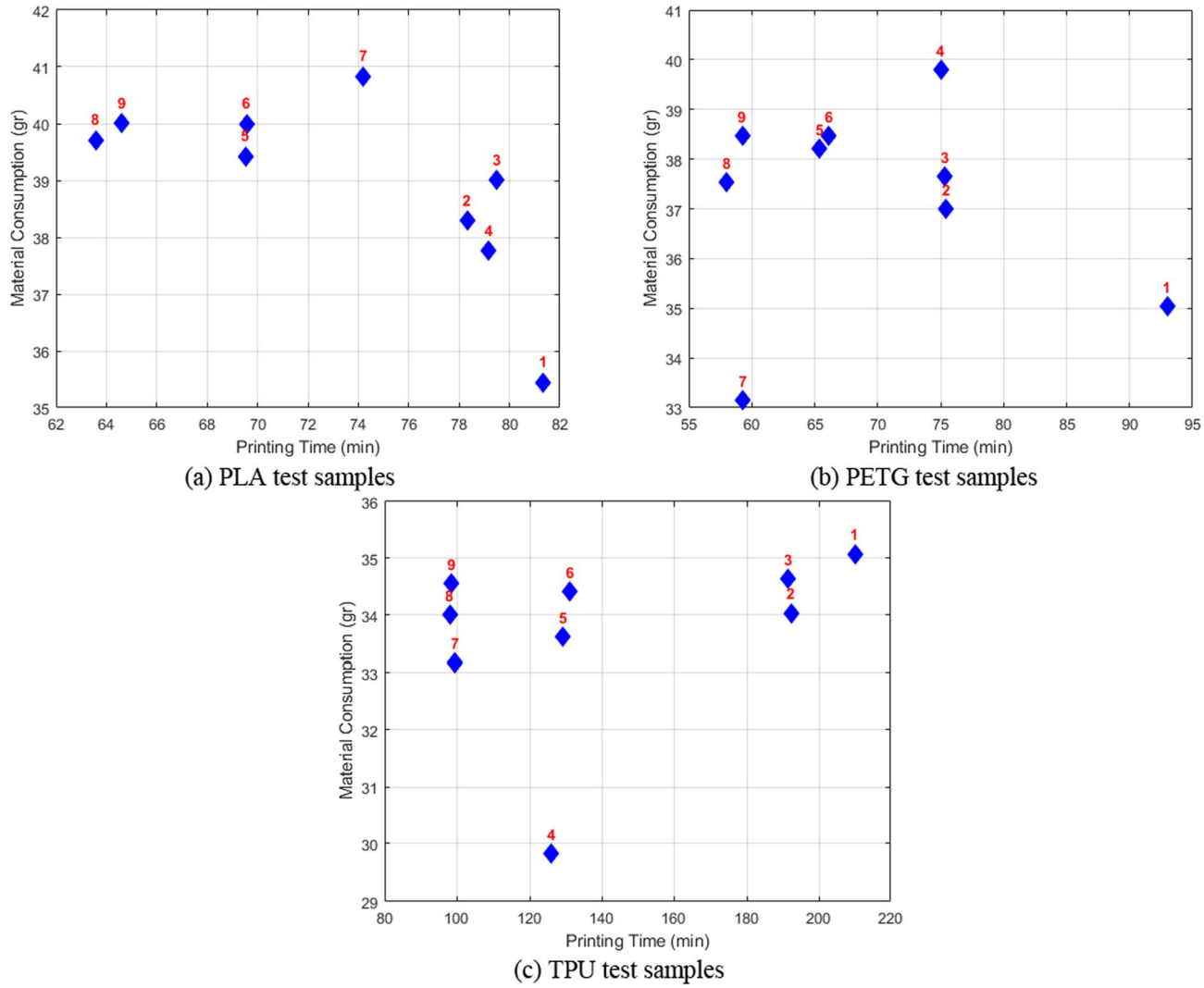

Fig. 4 Printing time and material consumption of PLA, PETG and TPU test samples

Table 4 Mean of diameter and standard deviation of the circular part

	Material type	Experiment number								
	PLA	*1*	*2*	*3*	*4*	*5*	*6*	*7*	*8*	*9*
30 mm diameter	Mean diameter (mm)	30.20	30.28	30.29	30.19	30.27	30.35	30.33	30.37	30.41
	Standard deviation (mm)	0.01	0.02	0.04	0.02	0.02	0.01	0.05	0.04	0.04
	PETG	*1*	*2*	*3*	*4*	*5*	*6*	*7*	*8*	*9*
30 mm diameter	Mean diameter (mm)	30.36	30.28	30.24	30.44	30.38	30.43	30.58	30.54	30.66
	Standard deviation (mm)	0.05	0.04	0.03	0.04	0.02	0.05	0.04	0.05	0.04
	TPU	*1*	*2*	*3*	*4*	*5*	*6*	*7*	*8*	*9*
30 mm diameter	Mean diameter (mm)	30.37	30.26	30.41	30.54	30.73	30.99	31.15	30.67	30.95
	Standard deviation (mm)	0.04	0.01	0.03	0.02	0.04	0.05	0.03	0.02	0.05

distance and standard deviation values of the triangular and pentagonal parts on the x–y axis. The low standard deviation values obtained prove that the production process is repeatable and reliable. These results show that the developed implant models are suitable for clinical applications and can provide consistent results.

Table 5 Mean of distance and standard deviation in the x-axis of polygonal parts

	Material type	Experiment number								
	PLA	*1*	*2*	*3*	*4*	*5*	*6*	*7*	*8*	*9*
15.14 mm triangle	Mean diameter (mm)	15.21	15.23	15.20	15.26	15.25	15.24	15.30	15.35	15.37
	Standard deviation (mm)	0.01	0.02	0.01	0.03	0.04	0.03	0.04	0.05	0.05
	PETG	*1*	*2*	*3*	*4*	*5*	*6*	*7*	*8*	*9*
15.14 mm triangle	Mean diameter (mm)	15.23	15.28	15.22	15.29	15.27	15.32	15.34	15.37	15.36
	Standard deviation (mm)	0.01	0.03	0.02	0.03	0.03	0.04	0.04	0.05	0.04
	TPU	*1*	*2*	*3*	*4*	*5*	*6*	*7*	*8*	*9*
15.14 mm triangle	Mean diameter (mm)	15.25	15.27	15.24	15.28	15.29	15.34	15.35	15.36	15.38
	Standard deviation (mm)	0.02	0.03	0.01	0.03	0.03	0.04	0.04	0.05	0.05
	PLA	*1*	*2*	*3*	*4*	*5*	*6*	*7*	*8*	*9*
26.45 mm pentagon	Mean diameter (mm)	26.51	26.49	26.52	26.54	26.53	26.56	26.53	26.57	26.58
	Standard deviation (mm)	0.01	0.02	0.01	0.04	0.03	0.04	0.03	0.05	0.05
	PETG	*1*	*2*	*3*	*4*	*5*	*6*	*7*	*8*	*9*
26.45 mm pentagon	Mean diameter (mm)	26.52	26.56	26.53	26.58	26.57	26.59	26.58	26.61	26.64
	Standard deviation (mm)	0.01	0.03	0.02	0.04	0.02	0.04	0.04	0.04	0.05
	TPU	*1*	*2*	*3*	*4*	*5*	*6*	*7*	*8*	*9*
26.45 mm pentagon	Mean diameter (mm)	26.59	26.62	26.69	26.61	26.63	26.64	26.65	26.68	26.69
	Standard deviation (mm)	0.01	0.02	0.04	0.03	0.03	0.04	0.04	0.05	0.05

Table 6 Mean of distance and standard deviation in the y-axis of polygonal parts

	Material type	Experiment number								
	PLA	*1*	*2*	*3*	*4*	*5*	*6*	*7*	*8*	*9*
22.5 mm triangle	Mean diameter (mm)	22.51	22.61	22.57	22.83	22.61	22.64	22.63	22.71	22.64
	Standard deviation (mm)	0.02	0.02	0.02	0.05	0.01	0.04	0.03	0.04	0.03
	PETG	*1*	*2*	*3*	*4*	*5*	*6*	*7*	*8*	*9*
22.5 mm triangle	Mean diameter (mm)	22.62	22.64	22.58	22.93	22.65	22.72	22.66	22.75	22.65
	Standard deviation (mm)	0.02	0.02	0.02	0.05	0.02	0.04	0.03	0.05	0.03
	TPU	*1*	*2*	*3*	*4*	*5*	*6*	*7*	*8*	*9*
22.5 mm triangle	Mean diameter (mm)	22.59	22.68	22.61	22.95	22.73	22.75	22.69	22.78	22.81
	Standard deviation (mm)	0.01	0.02	0.02	0.05	0.03	0.04	0.02	0.04	0.05
	PLA	*1*	*2*	*3*	*4*	*5*	*6*	*7*	*8*	*9*
27.14 mm pentagon	Mean diameter (mm)	27.20	27.25	27.30	27.31	27.26	27.31	27.36	27.35	27.42
	Standard deviation (mm)	0.01	0.02	0.03	0.03	0.02	0.03	0.05	0.04	0.05
	PETG	*1*	*2*	*3*	*4*	*5*	*6*	*7*	*8*	*9*
27.14 mm pentagon	Mean diameter (mm)	27.24	27.37	27.31	27.32	27.36	27.40	27.55	27.48	27.44
	Standard deviation (mm)	0.01	0.03	0.02	0.02	0.03	0.03	0.05	0.04	0.05
	TPU	*1*	*2*	*3*	*4*	*5*	*6*	*7*	*8*	*9*
27.14 mm pentagon	Mean diameter (mm)	27.40	27.48	27.57	27.53	27.50	27.60	27.80	27.67	27.78
	Standard deviation (mm)	0.02	0.02	0.04	0.03	0.03	0.04	0.05	0.05	0.05

In addition to the measured and calculated average diameter and standard deviation parameters, percentage dimensional changes were also calculated. Dimensional deviations of circular parts are shown in percentages in Fig. 5. The graph shows the dimensional deviations observed in circular biomedical implant parts manufactured using three different materials. Calculating percentage deviations is important in terms of allowing comparison of parts of different sizes and providing a more objective measure for evaluating the overall performance of the manufacturing process. PLA shows the lowest dimensional deviation, ranging from 0.5% to 1.5% among the materials. This demonstrates PLA's superior precision and consistency, making it an ideal choice for applications where precision is crucial. PETG exhibits moderate

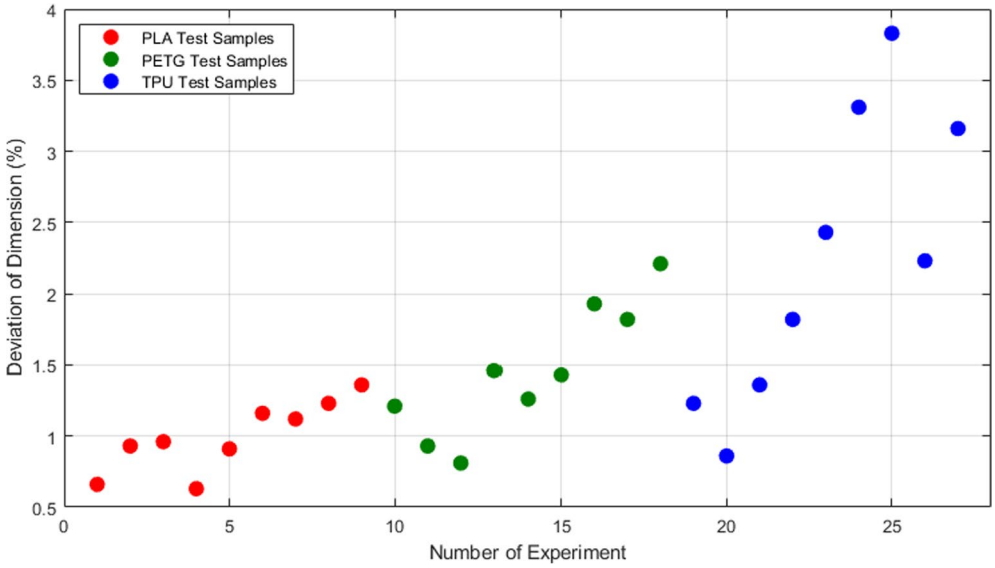

Fig. 5 Dimensional deviations of circular biomedical implant parts

deviations, ranging from 1% to 2.5%. Although less precise than PLA, PETG offers a balance between mechanical properties and dimensional stability, making it suitable for less critical applications. TPU shows the highest dimensional variability, ranging from 2% to 3.5%. This is likely due to the elastic and flexible nature of TPU.

The dimensional deviations of the triangular biomedical implant parts in the X and Y axes highlight significant differences in material performance (Fig. 6). In the X-axis measurements, PLA demonstrates superior dimensional accuracy and stability, showing the lowest deviations ranging from 0.4% to 0.8%. PETG demonstrates moderate accuracy, showing slightly higher deviations between 0.6% and 1.2%. On the other hand, TPU records the highest deviations between 1.0% and 1.6%, reflecting the difficulties in maintaining dimensional stability due to its elastic structure. Similarly, in the Y-axis measurements, PLA proves to be the most consistent material again with deviations in the same range (0.4% to 0.8%), confirming its reliability in both dimensions. PETG continues to show moderate deviations ranging from 0.6% to 1.4%, while TPU shows the highest variability, reaching deviations up to 2.0%. These findings indicate that PLA is the most suitable material for applications requiring high dimensional accuracy in triangular

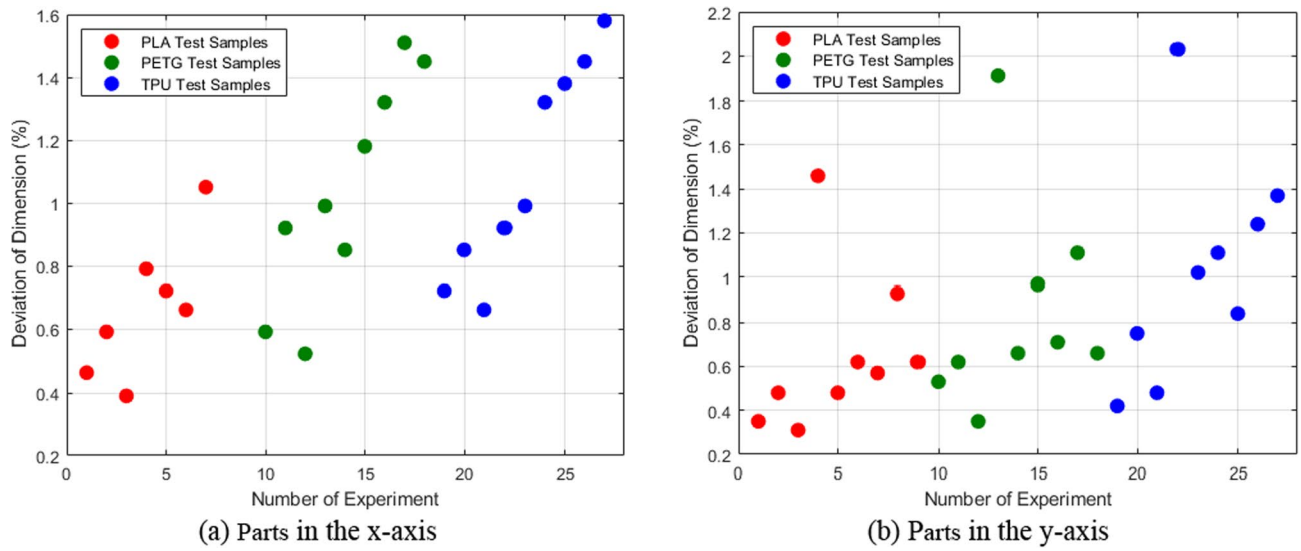

Fig. 6 Dimensional deviations of triangle biomedical implant parts in the x and y axes

geometries, while PETG offers a balanced alternative for less critical applications. Despite its higher dimensional deviations, TPU may be preferred for applications that prioritize flexibility over precision.

Figure 7 illustrates the dimensional deviations of pentagonal biomedical implant parts in the X and Y axes for PLA, PETG, and TPU materials. In the X-axis measurements, PLA exhibits the lowest deviations, ranging from 0.2% to 0.5%, demonstrating exceptional dimensional precision and stability. PETG shows moderate deviations between 0.3% and 0.7%, balancing accuracy and versatility. TPU, however, records the highest deviations, ranging from 0.6% to 0.9%, likely due to its elastic and flexible properties, which pose challenges in maintaining dimensional stability. Similarly, in the Y-axis measurements, PLA maintains superior performance with deviations between 0.3% and 0.8%, confirming its reliability for precise applications. PETG shows slightly increased variability in the Y-axis, with deviations ranging from 0.4% to 1.2%, while TPU exhibits the highest deviations, ranging from 0.8% to 2.0%.

Dimensional deviation analysis of biomedical implant samples in different geometries reveals important results on a material basis. PLA material exhibits superior performance by showing the lowest dimensional deviations in all geometric structures. It provides the most consistent results with deviations ranging from 0.5–1.5% in circular structures, 0.4–0.8% in triangular geometries and 0.2–0.8% in pentagonal structures. The very low deviation values such as 0.2% that PLA shows especially in pentagonal geometries prove that the material can be manufactured with high precision even in complex geometries. This feature makes PLA an ideal material for biomedical implant applications that require particularly precise anatomical adaptation. PETG exhibits moderate performance in all geometries. It exhibits deviations ranging from 1.0–2.5% in circular structures, 0.6–1.4% in triangular geometries and 0.3–1.2% in pentagonal structures. The fact that PETG's deviation values vary depending on the geometry reveals the sensitivity of the material to processing parameters. However, these deviations are still within acceptable limits, making PETG a suitable alternative for applications requiring medium-level precision. TPU shows the highest dimensional deviations in all geometries due to its elastic structure. It exhibits deviations ranging from 2.0–3.5% in circular structures, 1.0–2.0% in triangular geometries, and 0.6–2.0% in pentagonal structures The higher deviation values observed in circular geometries with TPU indicate that the material's elasticity causes more significant deformation on curved surfaces than on linear features. However, despite these high deviation values, TPU's elastic properties can provide advantages for some specific biomedical applications.

Pentagonal structures consistently show smaller deviation values across all materials, compared to the higher deviations found in circular geometries. The reason is that 3D printing systems allow for greater control in producing straight edges and angular geometries. This information highlights the impact of geometry selection on dimensional accuracy in implant design. These results show that material selection in biomedical implant design should be considered together with geometry. PLA is preferred in applications requiring high precision, while design tolerances should be determined accordingly by considering the high deviation values of TPU in applications requiring flexibility. PETG offers a balanced alternative between the two extremes with its intermediate performance.

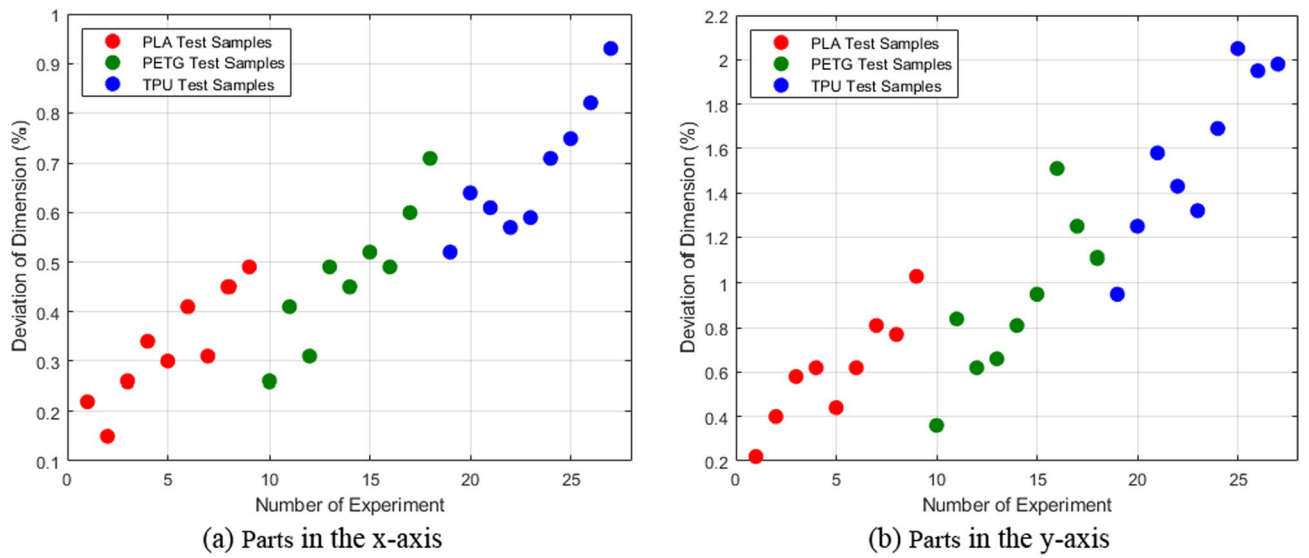

Fig. 7 Dimensional deviations of pentagon biomedical implant parts in the x and y axes

3.2 Evaluation of Taguchi Results

In this section, the analysis results of biomedical implant models fabricated with the FDM are given by Taguchi. This analysis process was performed using the surface roughness data in Table 3 and the dimensional accuracy data in Tables 4, 5 and 6. The Taguchi is a powerful statistical approach that provides optimization of process parameters using the S/N ratio. The higher the S/N ratio, the better the controllability of the process parameters. In the experimental studies, low dimensional deviation and roughness values mean high dimensional accuracy and surface quality of the part. In the study, material (PLA, PETG, and TPU), layer thickness (200 µm, 300 µm, 400 µm), infill density (%30, %60, %90), infill pattern (Zigzag, Cubic, Triangle), and wall thickness (1 mm, 2 mm, 3 mm) were used as printing parameters. Firstly, the relationship between the 3D printing parameters in the production of biomedical implants and the material consumption and printing time was investigated with Taguchi. Then, the dimensional accuracy and surface roughness of the geometric parts were analyzed.

3.2.1 Evaluation of Material Consumption and Printing Time

The effect of printing parameters on material consumption and printing time is given in Fig. 8. The best results in terms of material consumption were obtained with TPU material,

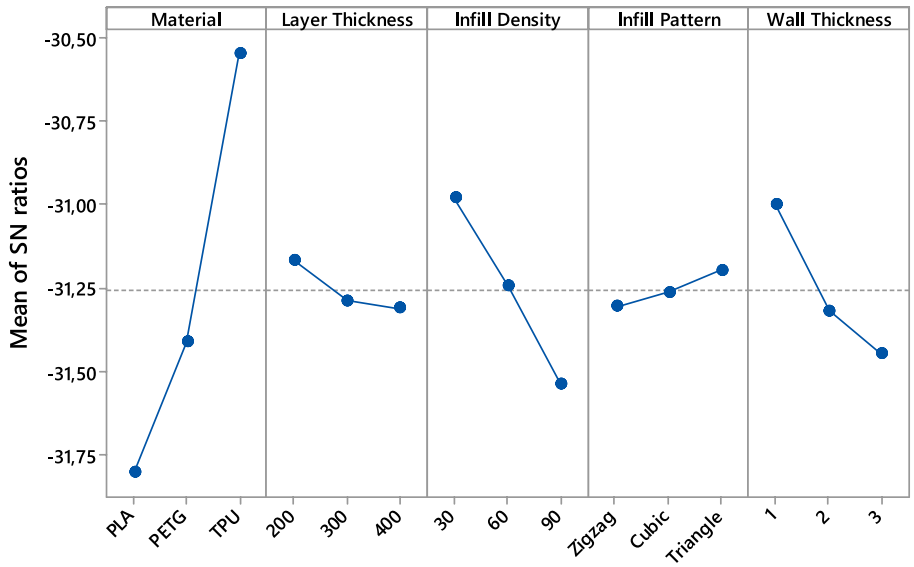

(a) material consumption

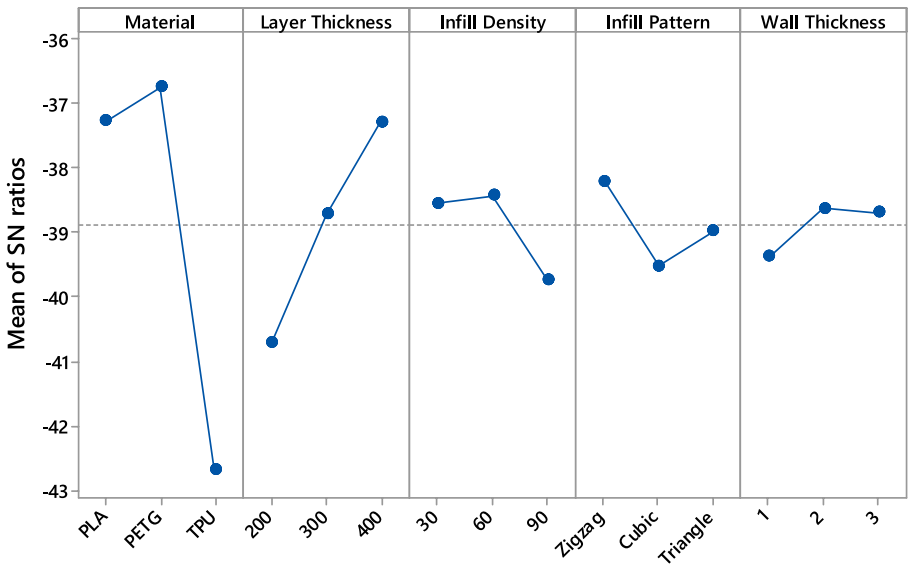

(b) printing time

Fig. 8 Main effects plot for SN ratios **a** material consumption **b** printing time

200 µm layer thickness, 30% infill density, Triangle infill pattern and 1 mm wall thickness parameters. This combination of parameters provides minimum material consumption (Fig. 8a). In terms of printing time, PETG material, 400 µm layer thickness, 60% infill density, Zigzag infill pattern and 2 mm wall thickness gave the most optimized results (Fig. 8b). In both graphs, increasing the infill density from 30 to 90% significantly increased material consumption and printing time.

The negative values of the S/N ratios in the graphs indicate that the "smaller is better" approach was used. In this approach, smaller S/N values indicate better results. In particular, the effect of infill density and wall thickness is clearly seen in the material consumption graph. In the printing time graph, the layer thickness has a significant effect, and the printing time decreases as the thickness increases. These analysis results provide important data for the optimum parameter selection in biomedical implant production. The Taguchi enables the identification of the optimal parameter combinations for minimizing material consumption and printing time.

3.2.2 Evaluation of Dimensional Accuracy

In this section, the dimensional accuracy of the geometric structures (circular, triangle, and pentagon) used in the production process of biomedical implants is examined using Taguchi results. Examining the dimensional accuracy of different geometric structures is of critical importance for the implant design and production process. Implants can be designed with varying geometries to match the specific anatomical requirements of different body regions. Therefore, the ability to produce implants with high dimensional accuracy in various geometries is a basic requirement for personalized implant production and a successful implantation process. The "smaller is better" approach was used for the dimensional accuracy analysis of the 30 mm diameter circular part shown in Fig. 9, as the aim is for the implant models to have the lowest dimensional deviation.

The optimum parameter combination for the highest dimensional accuracy of circular biomedical implant parts is determined as follows: PLA material (highest S/N ratio approximately 10.5), 200 µm layer thickness (S/N ratio approximately 7.5), 90% infill density (S/N ratio approximately 5), Cubic infill pattern (S/N ratio approximately 5) and 2 mm wall thickness (S/N ratio approximately 5). Material selection has a very significant effect on dimensional accuracy. A dramatic decrease in the S/N ratio is observed as we move from PLA to TPU. This shows that PLA has better dimensional stability due to its more rigid structure. Similarly, it is seen that dimensional accuracy decreases with increasing layer thickness. The S/N ratio decreases significantly as we move from 200 µm to 400 µm. In terms of infill density, it is observed that dimensional accuracy improves as the density increases. This can be explained by the fact that higher infill ratio provides better structural stability to the part. The Cubic pattern gives the best result in the infill pattern parameter, and 2 mm is the optimum value in wall thickness. To achieve high dimensional accuracy in circular biomedical implants, use PLA material with 200 µm layer thickness, 90% infill density, cubic infill pattern, and 2 mm wall thickness. This parameter combination provides the optimum conditions for the lowest dimensional deviation and the highest geometric accuracy.

Figure 10 shows the Taguchi results of the dimensional accuracy of the biomedical implant parts with triangular geometry along the x and y axes. The analysis was performed separately for the x-axis with a width of 15.14 mm

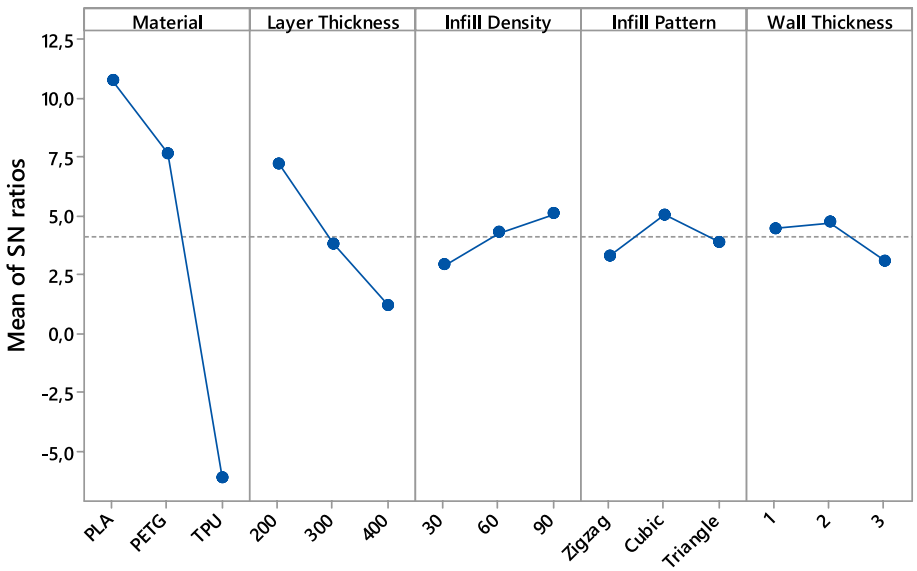

Fig. 9 Printing parameters vs SN ratios at different levels of variables for 30 mm diameter circular biomedical implant parts

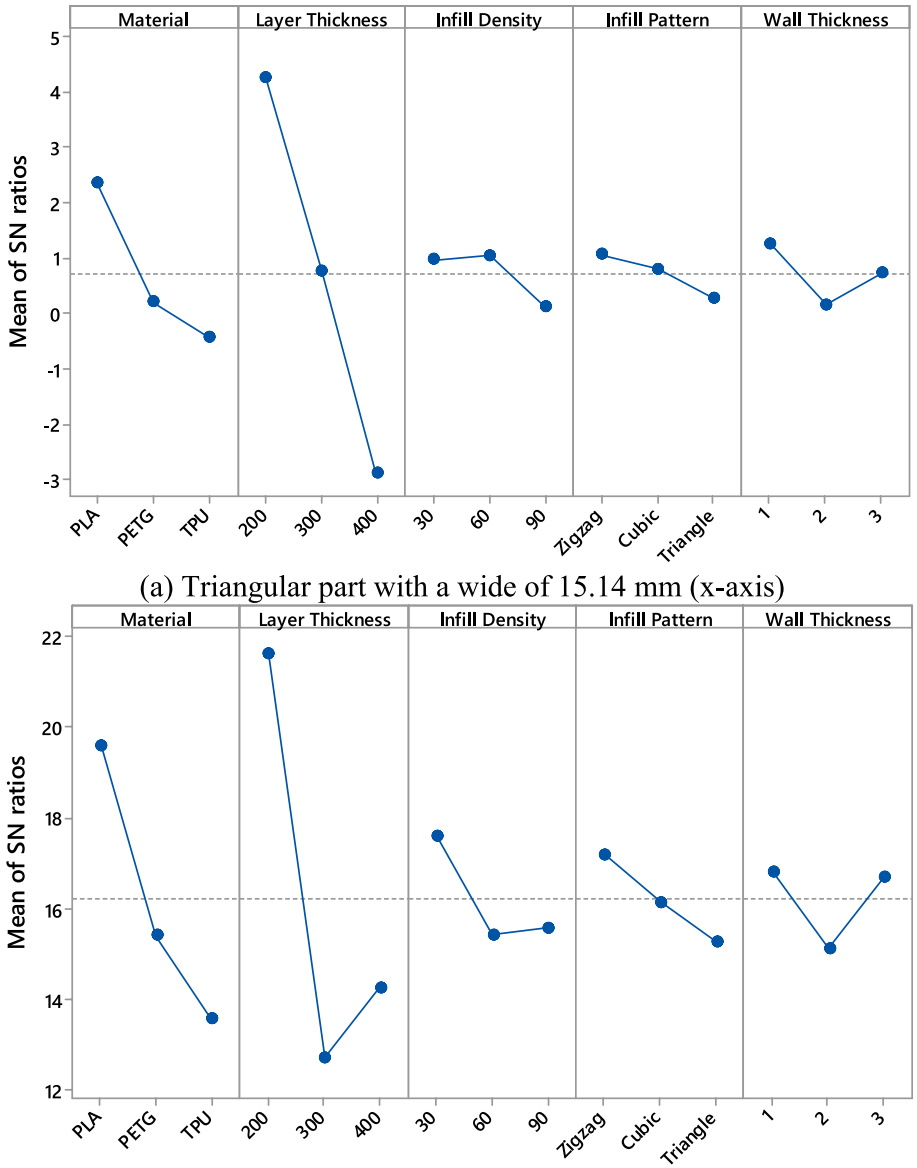

(a) Triangular part with a wide of 15.14 mm (x-axis)

(b) Triangular part with a wide of 22.5 mm (y-axis)

Fig. 10 Printing parameters vs SN ratios at different levels of variables for triangle biomedical implant parts in the x and y axes

and the y-axis with a width of 22.5 mm. When the results for the x-axis are examined, the optimum parameter combination for the highest dimensional accuracy is as follows: PLA material, 200 µm layer thickness, 30–60% infill density, Zigzag infill pattern, and 1 mm wall thickness. The dimensional accuracy decreases significantly with the increase of the layer thickness from 200 µm to 400 µm. When looking at the results for the y-axis (22.5 mm), a different trend is observed. The optimum parameters for the best dimensional accuracy in this axis were determined as: PLA material, 200 µm layer thickness, 30% infill density, Zigzag infill pattern, and 1 mm or 3 mm wall thickness. PLA material and 200 µm layer thickness give the best results in both axes, while S/N ratios in the y-axis are generally higher. This shows that the dimensional accuracy in the y-axis is better than in the x-axis. In addition, the effect of parameter changes on dimensional accuracy is more pronounced in the y-axis. For triangular biomedical implants, PLA material and 200 µm layer thickness are recommended for optimal production. However, the selection of other parameters should account for which axis has the most critical need for dimensional accuracy. These results emphasize the importance of axis-based optimization in the design and production process of triangular geometry implants.

Figure 11 shows the Taguchi results of the dimensional accuracy of biomedical implant parts with pentagonal geometry along the x and y axes. This analysis was evaluated separately for the x-axis with a width of 26.45 mm and the y-axis with a width of 27.14 mm. When the x-axis (26.45 mm) results are examined, the optimum parameter

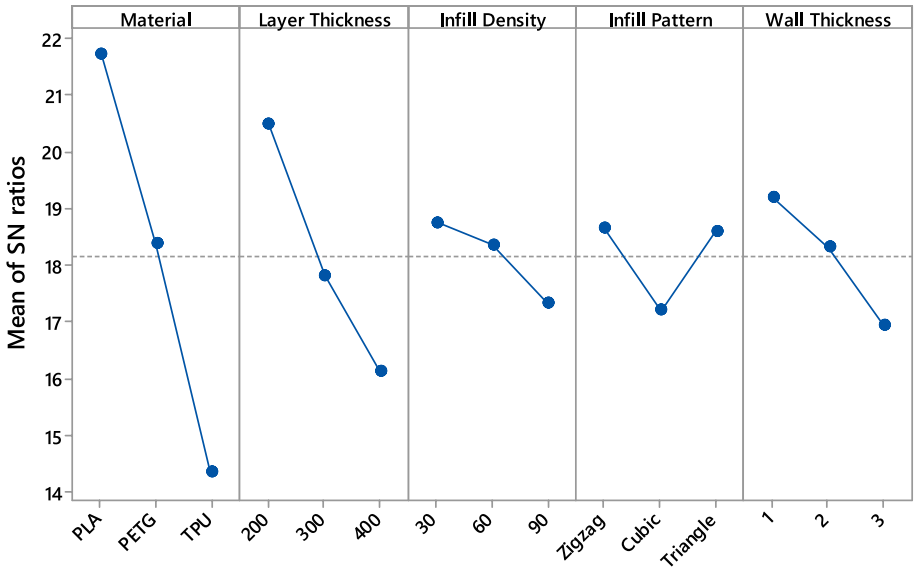

(a) Pentagonal part with a wide of 26.45 mm (x-axis)

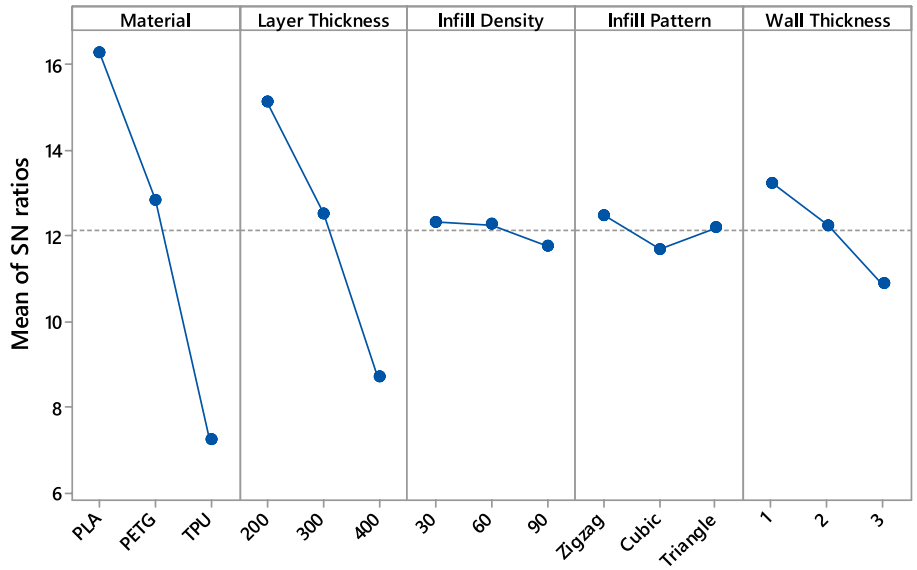

(b) Pentagonal part with a wide of 27.14 mm (y-axis)

Fig. 11 Printing parameters vs SN ratios at different levels of variables for pentagon biomedical implant parts in the x and y axes

combination for the highest dimensional accuracy is as follows: PLA material (highest S/N ratio), 200 µm layer thickness, 30% infill density, Cubic infill pattern and 2 mm wall thickness. The effect of the material selection is particularly striking; it is seen that the dimensional accuracy decreases significantly in the transition from PLA to TPU. In the y-axis (27.14 mm) results, a similar trend is seen, but there are some differences. The optimum parameters for the best dimensional accuracy in this axis are determined as: PLA material, 200 µm layer thickness, 60% infill density, Zigzag infill pattern and 1 mm wall thickness. It is noteworthy that the infill density in the y-axis should be higher than the x-axis.

The most important point common to both axes is that PLA material and low layer thickness (200 µm) give the best results. Dimensional accuracy decreases significantly in both axes with increasing layer thickness (up to 400 µm). This situation emphasizes the critical importance of thin layer thickness for precise production of pentagonal geometry parts. In terms of infill density, 30% for the x-axis and 60% for the y-axis give optimum results, while Cubic for the x-axis and Zigzag pattern for the y-axis provided better results in terms of infill pattern. This difference is due to the structural properties of the pentagonal geometry in different axes. As a result, axis-based optimization is important in the production of pentagonal geometry biomedical implant

parts. PLA material and low layer thickness should be preferred for both axes, but which axis is more critical should be taken into consideration in the selection of infill density and infill pattern. These analysis results are an important guide for the optimization of parameters required for the precise production of pentagonal geometry implants.

When the Taguchi results of biomedical implants with circular, triangular and pentagonal geometries are examined, material selection is the most critical parameter on dimensional accuracy. In all geometries, PLA material provided the highest dimensional accuracy thanks to its rigid structure and low thermal expansion coefficient. While PETG showed the second-best performance, TPU had the lowest dimensional accuracy because of its flexible structure. Therefore, it is important to prefer PLA in biomedical implant applications that require high precision. When evaluated in terms of layer thickness, 200 µm thickness gave the best results in all geometries, and dimensional accuracy decreased significantly as the thickness increased to 400 µm. The infill density parameter varied depending on the geometry, with a infill density of 90% in circular parts and 30–60% in triangular and pentagonal parts giving optimal results. In terms of infill pattern, Cubic pattern stood out in circular parts, while Zigzag and Cubic patterns performed better in triangular and pentagonal parts. The circular geometry reached the highest dimensional accuracy values due to its symmetrical structure and the absence of corners. In the triangular geometry, significant differences were observed between the x and y axes, and higher S/N ratios were obtained especially in the y-axis. On the other hand, pentagonal geometry showed differences between the axes because of its more complex structure, and parameter optimization became more critical.

Considering all these results, it is recommended to use PLA material and 200 µm layer thickness for high dimensional accuracy in biomedical implant production, and to select the infill density and infill pattern specific to the geometry. In addition, axis-based optimization should be considered depending on the complexity of the geometry to be produced. These analysis results clearly demonstrate the importance of geometry-based parameter optimization in biomedical implant production and the critical role of material selection. In future implant design and production studies, optimizing these parameters will form the basis to produce more successful and sensitive implants.

3.2.3 Evaluation of Surface Roughness

In biomedical implants, surface roughness is critical for the implant-tissue interaction, cell adhesion, and biocompatibility. Low surface roughness reduces the risk of infection, accelerates tissue healing, and provides better integration at the implant-tissue interface. In addition, poor surface quality positively affects the mechanical performance and fatigue strength of the implant. Therefore, optimization of surface quality in implant production is one of the basic requirements for a successful implantation process. In this section, the surface roughness results of the Taguchi method used in the experimental design process of biomedical implants are given. A low Ra value means high surface quality. The average surface roughness values obtained from implant samples produced using FDM are presented in Table 3.

In the experimental process, the Taguchi L27 orthogonal array consisting of 27 separate experiments was used. The surface roughness was measured three times for each sample and the average value is included in the table. The "smaller is better" approach was applied to determine the parameter settings that gave the lowest surface roughness value. In this study, the surface roughness values of the implant varied between 12.32 µm-38.25 µm, and the lowest value was observed in Experiment 3. In this experiment, the printing parameters were set as follows: PLA material, 200 µm layer thickness, 30% infill density, Zigzag infill pattern and 3 mm wall thickness.

Figure 12 shows the S/N ratios curves for surface roughness. The results indicate that material selection is the most critical parameter influencing the surface roughness of biomedical implant parts. The optimum parameter combination for the best surface quality was determined as: PLA material, 200 µm layer thickness, 90% infill density, Triangle infill pattern and 3 mm wall thickness. This parameter combination provides optimal conditions to achieve the desired low roughness values on implant surfaces. When the material performances were compared, PLA had the highest S/N ratio and provided the lowest surface roughness. While PETG showed a moderate performance, TPU caused the highest surface roughness with the lowest S/N ratio. This superiority of PLA is due to the material's more rigid structure, stable behavior during printing, biodegradable feature and low toxicity level. When the layer thickness parameter is examined, it is seen that 200 µm thickness provides the best surface quality, while the surface quality decreases significantly with increasing thickness. The lowest S/N ratio observed at 400 µm layer thickness shows that thick layers increase surface roughness. In the infill density, it was observed that 90% provides the best surface quality and the surface quality improves as the density increases (from 30 to 90%). The best result of the Triangle pattern in terms of infill pattern shows that the internal structure created by this pattern positively affects the surface quality, while the optimum value of 3 mm in wall thickness proves that thick walls increase surface stability. PETG and TPU should be preferred in implant production only in case of special requirements. As a result, it is important to use PLA material, prefer low layer thickness and select appropriate infill parameters in the fabrication of biomedical implants with high surface quality. This optimization is the factor that will directly affect the clinical

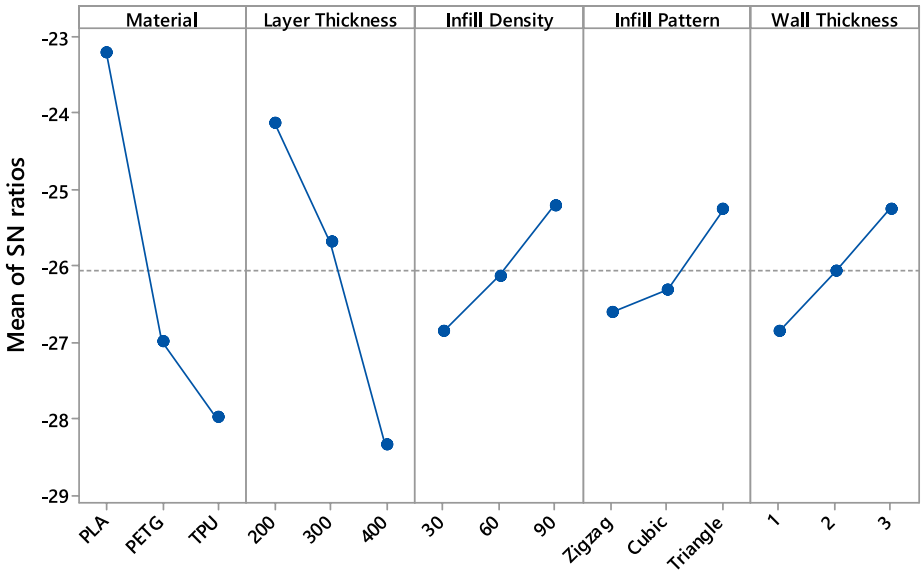

Fig. 12 Printing parameters vs SN ratios at different levels of variables for surface roughness of biomedical implant parts

performance and success rate of implants. The determined optimum parameter combination provides the most suitable conditions to achieve the desired low roughness values on implant surfaces.

3.3 Evaluation of ANOVA Results

In this section, the results of variance analysis (ANOVA) of biomedical implant models are examined. ANOVA is a statistical analysis method used to compare means between at least three groups and evaluates the relationship between categorical variables consisting of independent observations and quantitative variables consisting of numerical data. In the study, the printing parameters were used as material (PLA, PETG and TPU), layer thickness (200 µm, 300 µm, 400 µm), infill density (30%, 60%, 90%), infill pattern (Zigzag, Cubic, Triangular) and wall thickness (1 mm, 2 mm, 3 mm). The effects of these parameters on material consumption, printing time, dimensional accuracy and surface roughness were examined with ANOVA.

The use of ANOVA in biomedical implant models allows the systematic and statistically significant evaluation of the effects of different fabrication parameters on output quality. This is of critical importance for the optimization and standardization of the manufacturing process of implants. The contribution rates of the parameters were calculated based on the Adj SS values using the sum of squares, adjusted sum of squares, adjusted mean squares, F-value and p-value in ANOVA table. Expressing the contribution rates of the parameters as percentages enables a normalized comparison of data across different scales and units. This approach provides a direct understanding of which parameters are more effective on the process, making it easier to determine the areas that need to be focused on for the improvement of the production process.

3.3.1 Analysis of Material Consumption and Printing Time

Figure 13 shows the effect of printing parameters on material consumption and printing time for the samples. The contribution ratios of parameters on material consumption and printing time in the production of biomedical implant parts were examined. In terms of material consumption, material type has the highest contribution ratio (49.06%), followed by infill density (17.92%), wall thickness (13.56%), layer thickness (10.18%), and infill pattern (9.28%), respectively. When evaluating the printing time, material type again stands out with the highest contribution ratio (46.01%), while layer thickness (22.15%) rises to second place. These are followed by infill density (12.33%), infill pattern (11.54%), and wall thickness (7.97%). In the analysis performed at 95% confidence interval, all parameters with contribution ratios above 5% are shown to have statistically significant effects. These results indicate that material selection has a dominant effect on both material consumption and printing time, and layer thickness significantly influences the printing time.

3.3.2 Analysis of Dimensional Accuracy

The ANOVA was performed to evaluate the dimensional accuracy of biomedical implant parts, starting with circular geometry, followed by triangle and pentagon part analysis results. Figure 14 shows the contribution ratios of printing parameters for the 30 mm diameter circular model. According to the analysis results, material type emerges as the most influential parameter with the highest contribution ratio of 49.25%. Layer thickness shows the second-highest impact

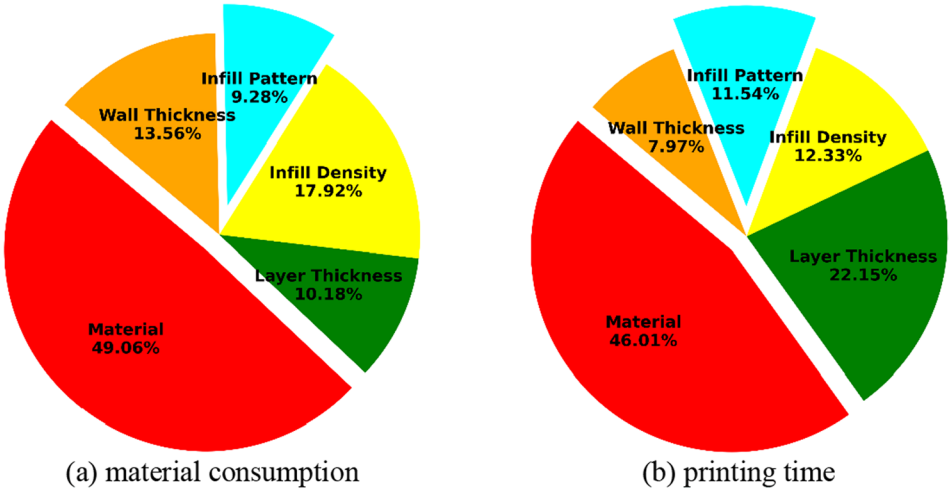

(a) material consumption (b) printing time

Fig. 13 Contribution of each parameter for **a** material consumption **b** printing time in biomedical implant parts

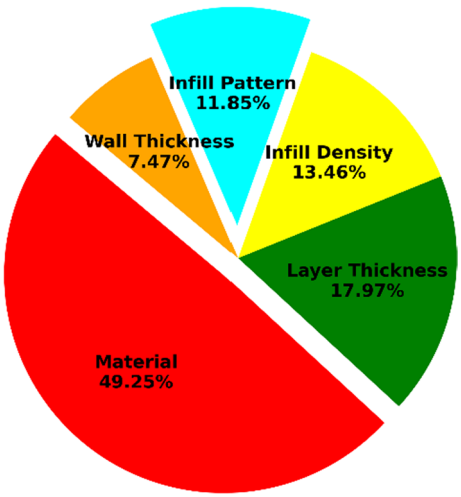

Fig. 14 Contribution of each parameter for 30 mm diameter circular biomedical implant parts

with a contribution ratio of 17.97%, followed by infill density at 13.46%. The infill pattern and wall thickness parameters demonstrate relatively lower effects, with contribution ratios of 11.85% and 7.47%, respectively. Since all parameters exhibit contribution ratios above 5% at the 95% confidence interval, they are considered statistically significant in affecting the dimensional accuracy of circular biomedical implant parts. Material selection plays a crucial role in achieving dimensional accuracy, while layer thickness also substantially influences the final dimensions of the circular parts.

Figure 15 presents the ANOVA results showing the contribution ratios of printing parameters for triangle biomedical implant parts in both x and y axes. The analysis reveals notable differences between the two axes. In the x-axis, layer thickness demonstrates the highest contribution with 57.45%, followed by material type at 17.75%. The remaining parameters show lower contributions with

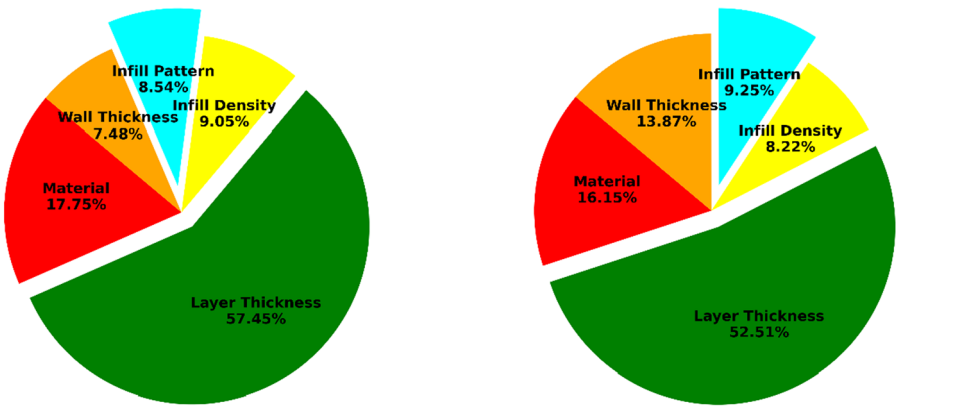

(a) Triangular part with a wide of 15.14 mm (x-axis) (b) Triangular part with a wide of 22.5 mm (y-axis)

Fig. 15 Contribution of each parameter for triangle biomedical implant parts in the x and y axes

infill density at 9.05%, infill pattern at 8.54%, and wall thickness at 7.48%. Similarly for the y-axis, layer thickness remains the dominant parameter with a slightly lower contribution ratio of 52.51%, while material type accounts for 16.15% of the variation. However, in the y-axis, wall thickness shows a higher contribution (13.87%) compared to the x-axis, followed by infill pattern (9.25%) and infill density (8.22%). All parameters in both axes maintain contribution ratios above 5%, indicating statistical significance at the 95% confidence interval. Layer thickness dominates dimensional accuracy in both axes, but wall thickness exhibits stronger influence on y-axis measurements compared to x-axis.

Figure 16 illustrates the ANOVA results displaying the contribution ratios of printing parameters for pentagon biomedical implant parts in both x and y axes. For the x-axis measurements, material type exhibits the highest contribution ratio at 44.58%, followed by layer thickness at 22.44%. Wall thickness shows a significant contribution of 16.45%, while infill pattern and infill density demonstrate lower effects at 9.58% and 6.95% respectively. In the y-axis analysis, a similar pattern emerges with material type maintaining the highest contribution at 43.52%, followed by layer thickness at 25.39%. Wall thickness continues to show substantial influence at 15.92%, while infill pattern (7.86%) and infill density (7.31%) maintain relatively lower contributions. Comparing the two axes, the contribution ratios remain consistent, with slight variations. The most notable difference is observed in layer thickness, which shows a higher contribution in the y-axis (25.39%) compared to the x-axis (22.44%). All parameters in both axes exceed the 5% contribution threshold, confirming their statistical significance at the 95% confidence interval. Compared to the triangle geometry, the pentagon shape demonstrates that material type is the leading factor in both axes, alongside considerable influences from layer thickness and wall thickness.

The comprehensive evaluation of dimensional accuracy ANOVA results across different geometries (circular, triangle, and pentagon) reveals several significant patterns and insights. Material type emerges as the most dominant parameter in circular (49.25%) and pentagon (44.58% x-axis, 43.52% y-axis) geometries, while showing lower influence in triangle geometry (17.75% x-axis, 16.15% y-axis). Layer thickness demonstrates its highest influence in triangle geometry (57.45% x-axis, 52.51% y-axis), maintains moderate influence in pentagon (22.44% x-axis, 25.39% y-axis), and shows significant effect in circular parts (17.97%). Wall thickness proves most influential in pentagon geometry (16.45% x-axis, 15.92% y-axis), shows increased importance in triangle y-axis (13.87%), but remains least influential in circular geometry (7.47%). The infill parameters (pattern and density) generally show lower contribution ratios across all geometries, with infill pattern ranging from 7.86% to 11.85% and infill density ranging from 6.95% to 13.46%. The analysis highlights that geometry significantly affects which parameters are most influential, with material type and layer thickness consistently emerging as the most critical parameters. All parameters maintain statistical significance (> 5% contribution) across all geometries. Geometric shapes exhibit different parameter sensitivities: layer thickness dominates triangle accuracy, while material type is most influential for pentagon and circular shapes.

3.3.3 Analysis of Surface Roughness

Figure 17 presents the ANOVA results for surface roughness parameters of biomedical implant parts. According to the analysis, layer thickness emerges as the most influential parameter with a contribution ratio of 30.95%, followed by material type which shows the second-highest impact at 31.28%. The infill density demonstrates a moderate influence with 14.39% contribution ratio, while infill pattern accounts

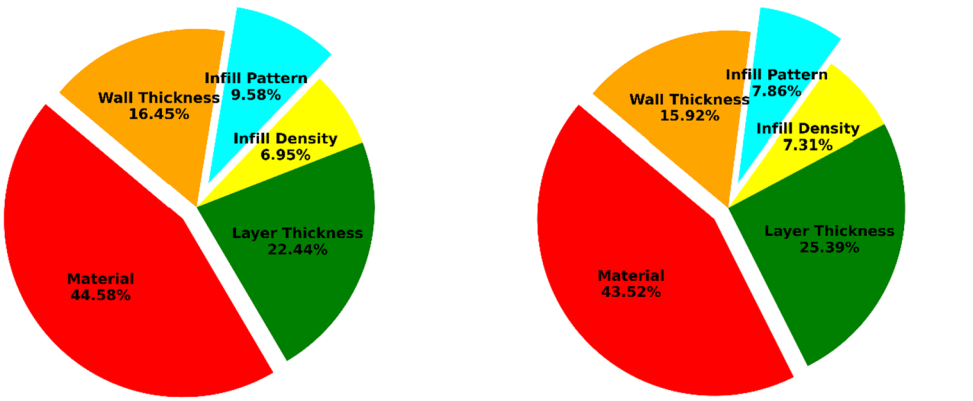

a) Pentagonal part with a wide of 26.45 mm (x-axis) (b) Pentagonal part with a wide of 27.14 mm (y-axis)

Fig. 16 Contribution of each parameter for pentagon biomedical implant parts in the x and y axes

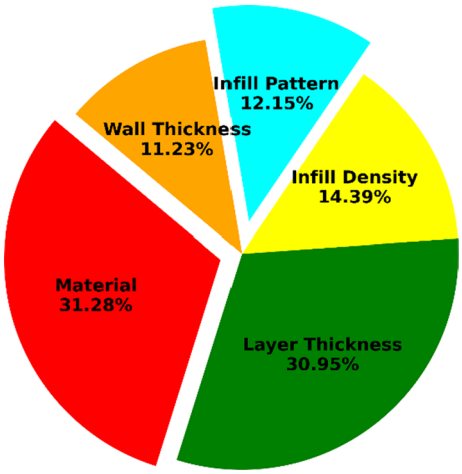

Fig. 17 Contribution of each parameter for surface roughness of biomedical implant parts

for 12.15% of the variation. Wall thickness shows the lowest effect among all parameters with an 11.23% contribution ratio. All parameters exhibit contribution ratios well above the 5% threshold, indicating their statistical significance at the 95% confidence interval. These results suggest that both layer thickness and material type play crucial roles in determining the surface roughness of biomedical implant parts, while the remaining parameters, although significant, have relatively less impact on the surface quality. Controlling layer thickness and selecting appropriate material types are essential factors for achieving desired surface roughness characteristics in biomedical implant manufacturing.

3.4 Artificial Neural Network Results

Predicting outcomes in advance is crucial for success in AM, as it enables accurate forecasting of process parameters and final outputs, leading to efficient resource utilization and significant time and cost savings. Today, various artificial intelligence techniques are used in AM technologies [52, 53]. Artificial neural networks (ANNs), modeled after the human brain, are widely regarded as a preferred method for simulating production processes. These systems could predict future situations by learning from existing data sets. ANNs are intelligent systems that can learn from experiences, just like biological systems, and apply this learning to new situations [54, 55]. Thanks to this feature, they can model complex relationships in AM and contribute to the optimization of process parameters. The success of the system is directly related to the quality and quantity of the data set used for training. ANNs trained with sufficient and accurate data can detect problems that may arise in the production process in advance and offer solution suggestions [56, 57].

In this study, an ANN model was developed to numerically predict the dimensional accuracy and surface quality of biomedical implant parts manufactured using FDM, one of the AM methods. The ANN implementation involved the creation of datasets designated for training, validation, and testing. A total of 216 experimental data points (8 outputs × 27 combinatorial points) were randomly distributed for ANN training (75%), validation (10%), and testing (15%). The training set included samples from each geometric configuration and material type, ensuring comprehensive coverage of the parameter space. The validation set was strategically selected to include boundary cases and mid-range values, while the testing set incorporated random samples across the full range of parameters. To assess dataset sufficiency, we conducted sensitivity analyses showing that increasing the dataset size beyond 216 points did not significantly improve model performance, suggesting adequate data representation. Cross-validation techniques were employed to verify that the model's performance remained consistent across different data subsets, confirming the robustness of the training process.

During the model development process, a feedforward neural network architecture was implemented in MATLAB and trained using the Levenberg–Marquardt algorithm. This algorithm was selected due to its ability to provide fast and stable results during ANN training. The model structure incorporated a single hidden layer with ten hidden neurons. The sigmoid activation function was chosen for both the hidden layer and output layer, ensuring effective signal processing throughout the network. The coefficient of determination (R^2) criterion was employed to evaluate the prediction performance. This statistical method is widely used in regression analysis to assess model performance, where an R^2 value of 1 indicates that the experimental data provides a perfect linear curve. The initial phase of the study focused on predicting the output parameters of material consumption and printing time in the 3D printing process. Subsequently, the dimensional accuracy of each geometric model and surface roughness values were predicted. The model's prediction performance was validated through comparison with experimental data.

3.4.1 ANN of Material Consumption and Printing Time

The provided figures demonstrate the correlation between actual and predicted values for two key parameters in AM: material consumption and printing time, using ANN predictions (Fig. 18). The material consumption prediction shows a strong correlation with an R^2 value of 0.9754, indicating that the ANN model explains approximately 97.54% of the variance in the data (Fig. 18a). The blue dots representing individual data points are closely clustered around the red regression line, demonstrating consistent prediction

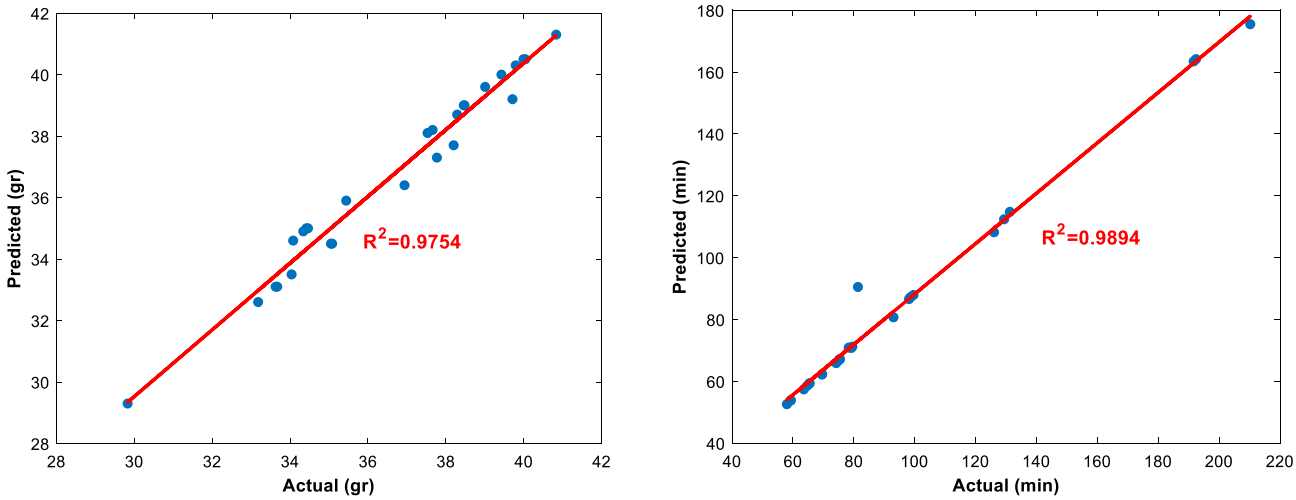

(a) material consumption (b) printing time

Fig. 18 Comparison of actual and predicted values with ANN for **a** material consumption **b** printing time

accuracy across the range of 29–41 g of material usage. Figure 18b displays an even stronger correlation for printing time predictions, with an R^2 value of 0.9894. This exceptionally high coefficient of determination suggests that the ANN model predicts printing time with remarkable accuracy across a wide range from approximately 50 to 220 min. The data points show minimal deviation from the regression line, particularly in the mid-range values. These results validate the effectiveness of the ANN model in predicting both material consumption and printing time parameters.

3.4.2 ANN of Dimensional Accuracy

Figure 19 illustrates the correlation between actual and predicted diameter measurements for 30 mm circular biomedical implants, using an ANN prediction. The analysis reveals a strong correlation with an R^2 value of 0.9628, indicating that the ANN accounts for approximately 96.28% of the variance in diameter predictions. The data points, spanning from approximately 30.2 mm to 31.2 mm, show a consistent distribution along the red regression line. This narrow range of variation demonstrates good dimensional accuracy in the manufacturing process. The clustering of points near the regression line indicates reliable prediction capabilities of the ANN for dimensional accuracy. This is particularly significant for implant applications, where precise dimensional control is critical for proper fit and functionality. While there are some minor deviations from the regression line, the overall trend shows that the ANN can effectively predict dimensional outcomes within acceptable tolerances for biomedical applications.

Figure 20 presents the correlation between actual and predicted dimensional measurements for triangular biomedical

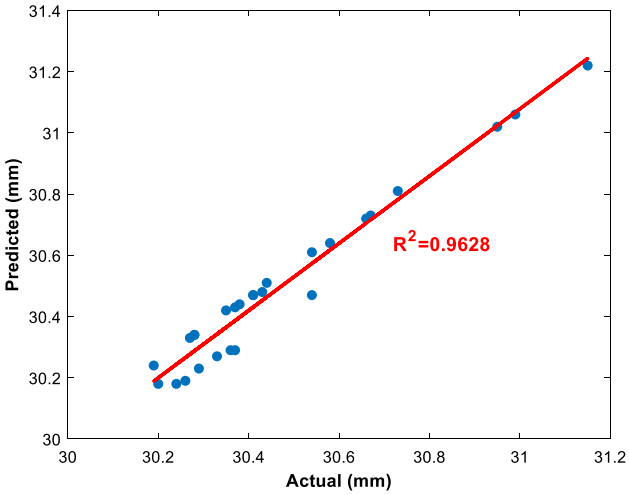

Fig. 19 Comparison of actual and predicted diameter values with ANN for 30 mm diameter circular biomedical implant parts

implant parts along both x and y axes, utilizing ANN prediction modeling. The graph for the x-axis measurements shows an excellent correlation with an R^2 value of 0.9765, while the y-axis measurements demonstrate a similarly strong correlation with an R^2 value of 0.9783. Both axes exhibit remarkably consistent prediction accuracy, with measurements ranging from approximately 15.2 to 15.4 mm for the x-axis and 22.5 to 23.0 mm for the y-axis. The data points in both graphs closely follow their respective regression lines, indicating highly reliable dimensional predictions by the ANN model. The narrow spread of measurements (approximately ± 0.1 mm for x-axis and ± 0.25 mm for y-axis) demonstrates excellent dimensional control in the manufacturing process. This level of accuracy is particularly crucial for

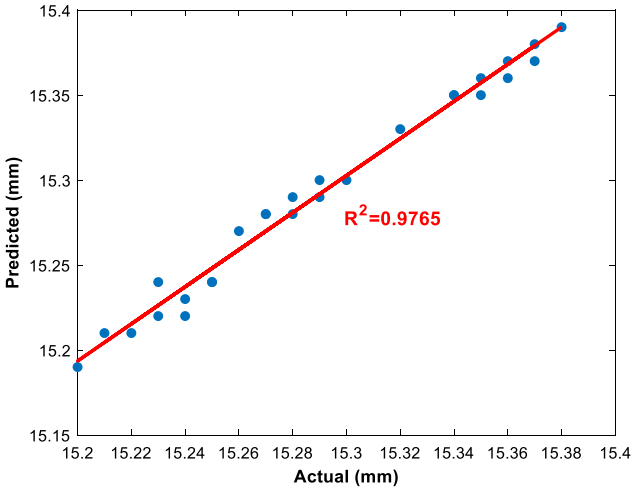

(a) Triangular part with a wide of 15.14 mm (x-axis)

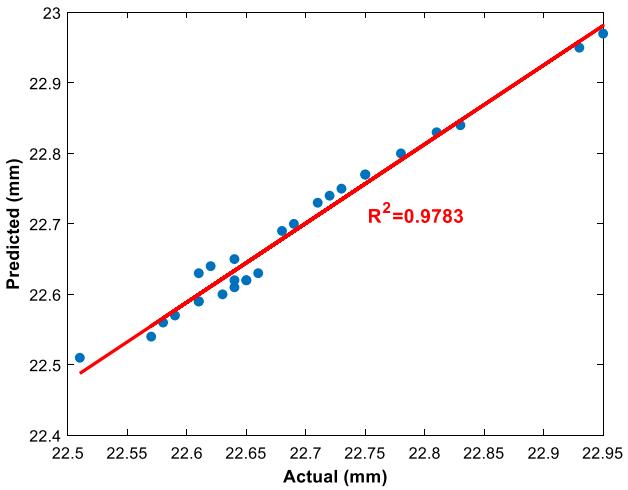

(b) Triangular part with a wide of 22.5 mm (y-axis)

Fig. 20 Comparison of the actual and predicted results with the ANN for triangle biomedical implant parts in the x and y axes

triangular biomedical implant parts, where geometric precision directly impacts the implant's fit and functionality. The nearly identical R^2 values between the x and y axes suggest that the ANN maintains consistent prediction capability regardless of the measurement direction. This uniformity in prediction accuracy across different geometric features is especially valuable for complex biomedical components that require precise dimensional control in multiple directions.

Figure 21 displays the correlation analysis between actual and predicted dimensional measurements for pentagonal biomedical implant parts along both x and y axes using ANN prediction modeling. For the x-axis measurements, the model demonstrates excellent predictive capability with an R^2 value of 0.9805. The data points range from approximately 26.45 to 26.75 mm, showing a tight clustering around the regression line. This high R^2 value indicates that the model accounts for 98.05% of the variance in the x-axis dimensional predictions. The y-axis measurements show an even stronger correlation with an R^2 value of 0.9766, covering a measurement range of approximately 27.2 to 27.9 mm. The data points exhibit remarkable adherence to the regression line, indicating highly accurate predictions across the entire measurement range. Both axes demonstrate exceptionally small deviations from their predicted values, with variations of approximately ± 0.15 mm for the x-axis and ± 0.35 mm for the y-axis. This level of precision

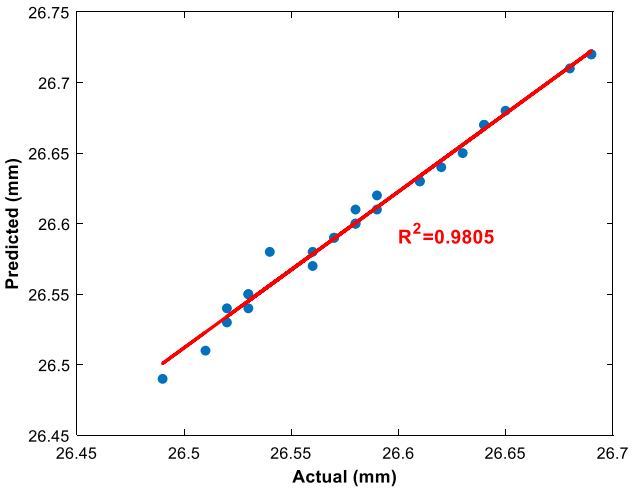

(a) Pentagonal part with a wide of 26.45 mm (x-axis)

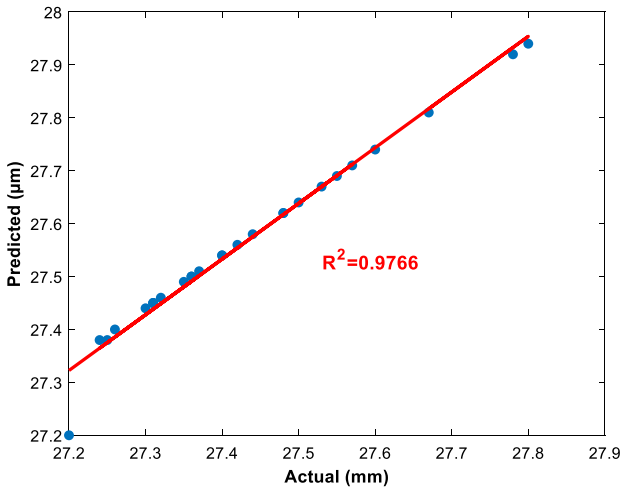

(b) Pentagonal part with a wide of 27.14 mm (y-axis)

Fig. 21 Comparison of the actual and predicted results with the ANN for pentagon biomedical implant parts in the x and y axes

is particularly important for pentagonal biomedical implant parts, where geometric accuracy in multiple directions is crucial for proper fitting and functionality. The consistently high R^2 values for both axes (0.9805 and 0.9766) validate the ANN model's reliability in predicting dimensional outcomes for complex geometric shapes like pentagons. This confirms the model's effectiveness for quality control and process optimization in the manufacturing of precision medical components with multiple critical dimensions.

Dimensional accuracy estimations performed using ANN have shown quite successful results for biomedical implant parts with different geometries. The fact that the R^2 values obtained for all geometric models are above 0.96 clearly shows the reliability and predictive power of the model. R^2 values of 0.9628 were obtained for circular implant parts, 0.9765 and 0.9783 for x and y axes for triangular implant parts, and 0.9805 and 0.9766 for x and y axes for pentagonal implant parts. The estimation error is below 5% for all geometries, which is quite acceptable for sensitive applications such as biomedical implants. The fact that the model can make consistent and high-accuracy estimations even in complex geometries such as pentagons and triangles, and that similar high accuracy rates are obtained in measurements on different axes, confirms that ANN can be used as a reliable estimation tool in biomedical implant production requiring dimensional precision. The developed ANN model is an effective tool for quality control and process optimization and provides significant advantages in terms of controlling dimensional accuracy, which is of critical importance in the production of biomedical implants.

3.4.3 ANN of Surface Roughness

The results of the ANN prediction model for the surface roughness of biomedical implant parts appear quite impressive (Fig. 22). The graph shows the relationship between the actual and predicted surface roughness values, and a high R^2 value of 0.9629 was obtained. The measured values cover a wide range from approximately 10 µm to 40 µm. The consistent distribution of data points around the regression line proves that the model can make reliable predictions even at different surface roughness levels. This result shows that the ANN model can be used as an effective tool in the surface quality control of biomedical implants. An accuracy rate of 96.29% in the prediction of surface quality, which is of critical importance for the biocompatibility and performance of implants, represents a very valuable success level in terms of optimizing the manufacturing process and quality control.

3.4.4 Discussion of ANN Results and Clinical Implications

The ANN model demonstrates excellent predictive capabilities across different geometric configurations and materials,

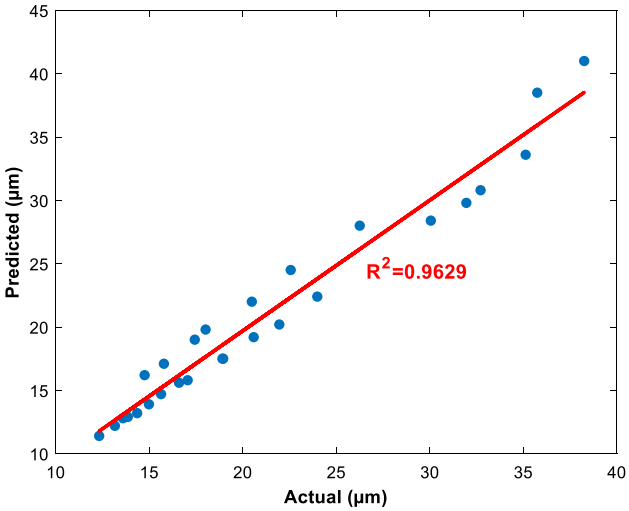

Fig. 22 Comparison of the actual and predicted results with the ANN for surface roughness of biomedical implant parts

with R^2 values consistently above 0.96. While these results are promising, the model's broader applicability and clinical implications deserve careful consideration. Successful prediction across basic geometric forms (circular, triangular, and pentagonal) suggests potential adaptability to various biomedical implant designs. However, the transition from these fundamental shapes to complex anatomical structures may present additional challenges. Although the model shows robust performance with PLA, PETG, and TPU, its applicability to other biocompatible materials such as PEEK or bioactive composites requires further evaluation to ensure broader utility in biomedical applications.

In the context of biomedical applications, precision requirements vary significantly depending on implant type and anatomical location. For load-bearing implants, dimensional accuracy typically requires tolerances within ± 0.1 mm, while surface roughness specifications often demand Ra values between 1–2 µm for optimal osseointegration. The current model's prediction accuracy ($R^2 > 0.96$) translates to maximum deviations of approximately ± 0.15 mm for dimensional measurements and ± 1.5 µm for surface roughness predictions. While these tolerances fall within acceptable ranges for many biomedical applications, certain high-precision applications may require even tighter controls.

The clinical implications of prediction deviations must be evaluated contextually. For instance, a 0.15 mm dimensional deviation might be acceptable for larger implants but could significantly impact the fit of micro-scale devices. Similarly, surface roughness variations of 1.5 µm could affect cell adhesion and tissue integration rates. To address these concerns, implementing additional safety factors in the manufacturing process is recommended when predicted

values approach critical thresholds. Furthermore, the model could be enhanced with confidence intervals to better inform quality control decisions in clinical applications.

Future improvements to enhance the model's utility in biomedical manufacturing applications could include the integration of real-time monitoring data to enable adaptive prediction during the manufacturing process. Additionally, incorporating material-specific behavioral models would enhance prediction accuracy for new biomaterials. The development of hybrid models combining ANN with other machine learning techniques could improve generalization capabilities. Furthermore, extending the model to include additional quality parameters such as mechanical properties and biocompatibility metrics would broaden its applicability. These potential improvements would maintain the model's current high prediction accuracy while expanding its capabilities to address more complex biomedical manufacturing challenges. The current results demonstrate that ANN modeling can serve as a valuable tool for quality control and process optimization in biomedical implant manufacturing, though continued refinement will further enhance its practical utility in clinical applications.

4 Conclusions

This study provides a comprehensive evaluation of the FDM process for prediction dimensional accuracy and surface quality in the production of biomedical implants. By employing the Taguchi method, ANOVA, and ANN, the research highlights critical insights into material selection, process parameters, and predictive modeling, offering a robust framework for precision manufacturing in biomedical applications. The findings underscore the importance of material selection, with PLA outperforming PETG and TPU in terms of dimensional accuracy and surface quality, thanks to its rigid structure, low thermal expansion coefficient, and excellent biocompatibility. Thin layer thickness (200 μm) emerged as a key parameter for achieving high precision and smooth surface finishes, while higher infill densities (60–90%) and thicker walls (2–3 mm) contributed to improved structural stability. Geometric effects were also significant, as circular shapes demonstrated higher dimensional accuracy compared to triangular and pentagonal geometries, indicating the need for axis-specific optimization in complex shapes. The Taguchi effectively identified optimal parameter combinations, while ANOVA revealed that material type and layer thickness were the most influential parameters, with contribution ratios of 49.25% and 30.95%, respectively. The developed ANN model achieved exceptional predictive accuracy ($R^2 > 0.96$) across all measured parameters including material consumption, printing time, dimensional accuracy, and surface roughness, marking a significant advancement in process prediction for biomedical applications. Unlike previous studies that typically focus on single geometric shapes or limited process parameters, our research uniquely investigates multiple geometries simultaneously, providing comprehensive insights into geometry-specific optimization requirements. The study's distinctive contribution lies in its systematic evaluation of three different biocompatible materials across various geometric configurations, establishing clear correlations between material properties and dimensional accuracy.

Several limitations and challenges were identified during the research that warrant further investigation. The model's current validation is limited to basic geometric shapes, and its applicability to complex anatomical structures requires additional study. The surface roughness predictions, while accurate within ± 1.5 μm, may need refinement for applications requiring sub-micron precision. Additionally, the current material selection, though representative of common biomedical materials, could be expanded to include high-performance polymers and composites. These limitations point to several promising directions for future research in the field of biomedical implant manufacturing. Extension of the methodology to include more complex, anatomically relevant geometries and investigation of their specific optimization requirements is essential. Integration of real-time monitoring and adaptive control systems could enhance manufacturing precision and reliability. Development of material-specific prediction models that account for the unique processing characteristics of advanced biomedical materials would broaden the application scope. Investigation of the relationship between predicted parameters and biological performance metrics, such as cell adhesion and tissue integration, would provide valuable insights for clinical applications. The methodology and findings presented in this study provide a robust framework for optimizing FDM parameters in biomedical implant manufacturing. The established correlations between process parameters and quality metrics, combined with the predictive capabilities of the ANN model, offer valuable tools for improving manufacturing efficiency and product quality. This integrated approach represents a significant step toward more reliable and efficient production of custom biomedical implants. The integration of statistical and machine learning techniques not only enhances the reliability of the manufacturing process but also supports the development of customized medical devices with superior precision and performance, though continued research is needed to address the identified limitations and expand the application scope. The insights gained from this study contribute substantially to the advancement of precision medicine through improved AM processes and enhanced implant performance, while also highlighting critical areas for future investigation and development in the field of biomedical manufacturing.

Funding Open access funding provided by the Scientific and Technological Research Council of Türkiye (TÜBİTAK). The author received no financial support for the research, authorship, and/or publication of this article.

Data and Code Availability All data underlying the results is available as part of the article and no additional source data are required.

Declarations

Conflict of interest The author declares no conflict of interest.

Ethical Approval The author declares that this study does not require ethical approval.

References

1. Kennedy, S. M., Amudhan, K., Britto, J. J. J., et al. (2024). Transformative applications of additive manufacturing in biomedical engineering: Bioprinting to surgical innovations. *Journal Medical Engineering Technology, 48*, 151–168. https://doi.org/10.1080/03091902.2024.2399017
2. Jang, J.-W., Min, K.-E., Kim, C., et al. (2023). Review: Scaffold characteristics, fabrication methods, and biomaterials for the bone tissue engineering. *International Journal of Precision Engineering and Manufacturing, 24*, 511–529. https://doi.org/10.1007/s12541-022-00755-7
3. Mobarak, M. H., Islam, M. A., Hossain, N., et al. (2023). Recent advances of additive manufacturing in implant fabrication – a review. *Applied Surface Science Advances, 18*, 100462. https://doi.org/10.1016/j.apsadv.2023.100462
4. Kumar, R., Kumar, M., & Chohan, J. S. (2021). The role of additive manufacturing for biomedical applications: A critical review. *Journal of Manufacturing Processes, 64*, 828–850. https://doi.org/10.1016/j.jmapro.2021.02.022
5. Wazeer, A., Das, A., Sinha, A., et al. (2023). Additive manufacturing in biomedical field: A critical review on fabrication method, materials used, applications, challenges, and future prospects. *Progess Additive Manufacturing, 8*, 857–889. https://doi.org/10.1007/s40964-022-00362-y
6. He, X., Zhang, K., Li, R., et al. (2024). Priority analysis and optimization for accuracy allocation of precision grinding machine considering manufacturing accuracy and cost. *International Journal of Precision Engineering and Manufacturing*. https://doi.org/10.1007/s12541-024-01117-1
7. Huang, Z., Jowers, C., Kent, D., et al. (2022). The implementation of Industry 4.0 in manufacturing: From lean manufacturing to product design. *International Journal of Advanced Manufacturing Technology, 121*, 3351–3367. https://doi.org/10.1007/s00170-022-09511-7
8. Blakey-Milner, B., Gradl, P., Snedden, G., et al. (2021). Metal additive manufacturing in aerospace: A review. *Materials and Design, 209*, 110008. https://doi.org/10.1016/j.matdes.2021.110008
9. Singh, A. B., Khandelwal, C., & Dangayach, G. S. (2024). Revolutionizing healthcare materials: Innovations in processing, advancements, and challenges for enhanced medical device integration and performance. *Journal Micromanufacturing*. https://doi.org/10.1177/25165984241256234
10. Alarifi, I. M. (2024). Revolutionising fabrication advances and applications of 3D printing with composite materials: A review. *Virtual and Physical Prototyping*. https://doi.org/10.1080/17452759.2024.2390504
11. Guzzi, E. A., & Tibbitt, M. W. (2020). Additive manufacturing of precision biomaterials. *Advances Material*. https://doi.org/10.1002/adma.201901994
12. Kim, K., & Baek, S. Y. (2023). Influence of counterpart material on fretting wear of FDM printed polylactic acid plates. *International Journal of Precision Engineering and Manufacturing, 24*, 1855–1863. https://doi.org/10.1007/s12541-023-00806-7
13. Borikar, G. P., Patil, A. R., & Kolekar, S. B. (2023). Additively manufactured lattice structures and materials: Present progress and future scope. *International Journal of Precision Engineering and Manufacturing, 24*, 2133–2180. https://doi.org/10.1007/s12541-023-00848-x
14. Martinez-Marquez, D., Gulati, K., Carty, C. P., et al. (2020). Determining the relative importance of titania nanotubes characteristics on bone implant surface performance: A quality by design study with a fuzzy approach. *Materials Science and Engineering C, 114*, 110995. https://doi.org/10.1016/j.msec.2020.110995
15. Singh, D., Singh, R., & Boparai, K. S. (2022). Investigations for surface roughness and dimensional accuracy of biomedical implants prepared by combining fused deposition modelling, vapour smoothing and investment casting. *Advance Material Processing Technology, 8*, 843–862. https://doi.org/10.1080/2374068X.2020.1835007
16. Galetto, M., Genta, G., Maculotti, G., & Verna, E. (2020). Defect probability estimation for hardness-optimised parts by selective laser melting. *International Journal of Precision Engineering and Manufacturing, 21*, 1739–1753. https://doi.org/10.1007/s12541-020-00381-1
17. Kumar, K. N., & Babu, P. D. (2024). Investigation on polymer hybrid composite through CO2 laser machining for precise machining conditions. *International Journal of Precision Engineering and Manufacturing, 25*, 1043–1061. https://doi.org/10.1007/s12541-023-00942-0
18. Pawlus, P., Reizer, R., & Wieczorowski, M. (2021). functional importance of surface texture parameters. *Materials (Basel), 14*, 5326. https://doi.org/10.3390/ma14185326
19. Fang, X., Luo, Q., Zhou, B., et al. (2020). Research progress of automated visual surface defect detection for industrial metal planar materials. *Sensors, 20*, 5136. https://doi.org/10.3390/s20185136
20. Pan, Y., Zhou, P., Yan, Y., et al. (2021). New insights into the methods for predicting ground surface roughness in the age of digitalisation. *Precision Engineering, 67*, 393–418. https://doi.org/10.1016/j.precisioneng.2020.11.001
21. Ulkir, O., & Akgun, G. (2024). Prediction of flexural strength with fuzzy logic approach for fused deposition modeling of polyethylene terephthalate glycol components. *Journal of Materials Engineering and Performance, 33*, 4367–4376. https://doi.org/10.1007/s11665-024-09291-z
22. Wu, L., Zhang, Y., Feng, Q., et al. (2024). A multifunctional flexible sensor with a 3D TPU fiber-based conductive network via in situ reduction of an AgNP layer. *ACS Sustainable Chemical*

Engineering, 12, 6111–6121. https://doi.org/10.1021/acssuschemeng.3c06811
23. Park, J.-H., Kim, S.-H., Park, J.-Y., et al. (2024). Prediction of microstructure and mechanical properties of ultrasonically treated PLA materials using convolutional neural networks. *International Journal of Precision Engineering and Manufacturing*. https://doi.org/10.1007/s12541-024-01081-w
24. Patel, R., Jani, S., & Joshi, A. (2023). Review on multi-objective optimization of FDM process parameters for composite materials. *International Journal on Interactive Design and Manufacturing, 17*, 2115–2125. https://doi.org/10.1007/s12008-022-01111-9
25. Kharate, N., Anerao, P., Kulkarni, A., & Abdullah, M. (2024). Explainable AI techniques for comprehensive analysis of the relationship between process parameters and material properties in FDM-based 3D-printed biocomposites. *Journal Manufacturing Material Processing, 8*, 171. https://doi.org/10.3390/jmmp8040171
26. Kam, M., İpekçi, A., & Şengül, Ö. (2023). Investigation of the effect of FDM process parameters on mechanical properties of 3D printed PA12 samples using Taguchi method. *Journal of Thermoplastic Composite Materials, 36*, 307–325. https://doi.org/10.1177/08927057211006459
27. Taşdemir, V. (2021). Investigation of dimensional integrity and surface quality of different thin-walled geometric parts produced via fused deposition modeling 3D printing. *Journal of Materials Engineering and Performance, 30*, 3381–3387. https://doi.org/10.1007/s11665-021-05809-x
28. Kechagias, J., Chaidas, D., Vidakis, N., et al. (2022). Key parameters controlling surface quality and dimensional accuracy: A critical review of FFF process. *Materials and Manufacturing Processes, 37*, 963–984. https://doi.org/10.1080/10426914.2022.2032144
29. Vinoth Babu, N., Venkateshwaran, N., Rajini, N., et al. (2022). Influence of slicing parameters on surface quality and mechanical properties of 3D-printed CF/PLA composites fabricated by FDM technique. *Materials Technology, 37*, 1008–1025. https://doi.org/10.1080/10667857.2021.1915056
30. Baraheni, M., Shabgard, M.R., Tabatabaee, A.M. (2024). Effects of FDM 3D printing parameters on PLA biomaterial components dimensional accuracy and surface quality. In: Proceedings of the Institution of Mechanical Engineers, Part C: Journal of Mechanical Engineering Science, 238:3864–3873. https://doi.org/10.1177/09544062231202142
31. Shahrubudin, N., Koshy, P., Alipal, J., et al. (2020). Challenges of 3D printing technology for manufacturing biomedical products: A case study of Malaysian manufacturing firms. *Heliyon, 6*, e03734. https://doi.org/10.1016/j.heliyon.2020.e03734
32. Hashmi, A. W., Mali, H. S., & Meena, A. (2023). A comprehensive review on surface quality improvement methods for additively manufactured parts. *Rapid Prototyping Journal, 29*, 504–557. https://doi.org/10.1108/RPJ-06-2021-0133
33. Borah, J., Chandrasekaran, M., & Selvarajan, L. (2023). Taguchi-based experimental investigation and modeling of 3D-printed PEEK parts as biomedical implants using fused deposition modeling for improving mechanical strength and surface quality. *Journal of Materials Engineering and Performance*. https://doi.org/10.1007/s11665-023-09036-4
34. Sai, T., Pathak, V. K., & Srivastava, A. K. (2020). Modeling and optimization of fused deposition modeling (FDM) process through printing PLA implants using adaptive neuro-fuzzy inference system (ANFIS) model and whale optimization algorithm. *J Brazilian Social Mechanical Science Engineering, 42*, 617. https://doi.org/10.1007/s40430-020-02699-3
35. Balasubramainian, N. K., Kothandaraman, L., Sathish, T., et al. (2024). Optimization of process parameters to minimize circularity error and surface roughness in fused deposition modelling (FDM) using Taguchi method for biomedical implant fabrication. *Advanced Manufacturing Polymer Composites Science*. https://doi.org/10.1080/20550340.2024.2406156
36. Sakthivel, N., Bramsch, J., Voung, P., et al. (2020). Investigation of 3D-printed PLA–stainless-steel polymeric composite through fused deposition modelling-based additive manufacturing process for biomedical applications. *Medical Devices Sensors*. https://doi.org/10.1002/mds3.10080
37. Gregory, D. A., Fricker, A. T. R., Mitrev, P., et al. (2023). Additive manufacturing of polyhydroxyalkanoate-based blends using fused deposition modelling for the development of biomedical devices. *J Funct Biomater, 14*, 40. https://doi.org/10.3390/jfb14010040
38. Mahmood, M. A., Visan, A. I., Ristoscu, C., & Mihailescu, I. N. (2020). Artificial neural network algorithms for 3D printing. *Materials (Basel), 14*, 163. https://doi.org/10.3390/ma14010163
39. Verma, D., Dong, Y., Sharma, M., & Chaudhary, A. K. (2022). Advanced processing of 3D printed biocomposite materials using artificial intelligence. *Materials and Manufacturing Processes, 37*, 518–538. https://doi.org/10.1080/10426914.2021.1945090
40. Ciccone, F., Bacciaglia, A., & Ceruti, A. (2023). Optimization with artificial intelligence in additive manufacturing: A systematic review. *Journal of the Brazilian Society of Mechanical Sciences and Engineering, 45*, 303. https://doi.org/10.1007/s40430-023-04200-2
41. Alnahdi, A. S., Khan, A., Gul, T., & Ahmad, H. (2024). Stagnation point nanofluid flow in a variable darcy space subject to thermal convection using artificial neural network technique. *Arabian Journal for Science and Engineering, 49*, 11309–11326. https://doi.org/10.1007/s13369-023-08697-6
42. Dejene, N. D., & Lemu, H. G. (2024). Characterisation and prediction of mechanical properties in laser powder bed fusion-printed parts: A comparative analysis using machine learning. *Material Technology*. https://doi.org/10.1080/10667857.2024.2419228
43. Teacher, M., & Velu, R. (2024). Additive Manufacturing of functionally graded materials: A comprehensive review. *International Journal of Precision Engineering and Manufacturing, 25*, 165–197. https://doi.org/10.1007/s12541-023-00864-x
44. Soon, C. F., Yee, S. K., Nordin, A. N., et al. (2024). Advancements in biodegradable printed circuit boards: Review of material properties, fabrication methods, applications and challenges. *International Journal of Precision Engineering and Manufacturing, 25*, 1925–1954. https://doi.org/10.1007/s12541-024-01027-2
45. Kahhal, P., Jo, Y.-K., & Park, S.-H. (2024). Recent progress in remanufacturing technologies using metal additive manufacturing processes and surface treatment. *International Journal of Precision Engineering and Manufacturing-Green Technology, 11*, 625–658. https://doi.org/10.1007/s40684-023-00551-2
46. Ranakoti, L., Gangil, B., Bhandari, P., et al. (2023). Promising role of polylactic acid as an ingenious biomaterial in scaffolds, drug delivery, tissue engineering, and medical implants: Research developments, and prospective applications. *Molecules, 28*, 485. https://doi.org/10.3390/molecules28020485
47. Thirugnanasambandam, A., Dutta, H., Gnanasagaran, C. L., & Kechagias, J. D. (2024). Development of 3D printed novel multipolymer component based on blended filaments of polylactic acid and polyethylene terephthalate glycol. *Progress in Additive Manufacturing*. https://doi.org/10.1007/s40964-024-00695-w
48. Desai, S. M., Sonawane, R. Y., & More, A. P. (2023). Thermoplastic polyurethane for three-dimensional printing applications: A review. *Polymers for Advanced Technologies, 34*, 2061–2082. https://doi.org/10.1002/pat.6041
49. Hisam, M. W., Dar, A. A., Elrasheed, M. O., et al. (2024). The versatility of the Taguchi method: Optimizing experiments across

diverse disciplines. *Journal Statistical Theory Applied, 23*, 365–389. https://doi.org/10.1007/s44199-024-00093-9
50. Uludag, M., & Ulkir, O. (2024). Optimizing surface roughness in soft pneumatic gripper fabricated via FDM: Experimental investigation using Taguchi method. *Multidiscipline Modeling in Materials and Structures, 20*, 211–225. https://doi.org/10.1108/MMMS-09-2023-0313
51. Ulkir, O., & Akgun, G. (2023). Predicting and optimising the surface roughness of additive manufactured parts using an artificial neural network model and genetic algorithm. *Science and Technology of Welding and Joining, 28*, 548–557. https://doi.org/10.1080/13621718.2023.2200572
52. Arivazhagan, A., Mani, K., Kamarajan, B. P., et al. (2024). Enhancing biocompatibility and mechanical properties of additively manufactured porous gyroid Ti–6Al–4V implants through hydroxyapatite infiltration. *International Journal of Precision Engineering and Manufacturing, 25*, 2177–2189. https://doi.org/10.1007/s12541-024-01046-z
53. Rahman, M. A., Saleh, T., Jahan, M. P., et al. (2023). Review of intelligence for additive and subtractive manufacturing: Current status and future prospects. *Micromachines, 14*, 508. https://doi.org/10.3390/mi14030508
54. Ibrahim, M., Haider, A., Lim, J. W., et al. (2024). Artificial neural network modeling for the prediction, estimation, and treatment of diverse wastewaters: A comprehensive review and future perspective. *Chemosphere, 362*, 142860. https://doi.org/10.1016/j.chemosphere.2024.142860
55. Alhamrouni, I., Abdul Kahar, N. H., Salem, M., et al. (2024). A comprehensive review on the role of artificial intelligence in power system stability, control, and protection: Insights and future directions. *Applied Sciences, 14*, 6214. https://doi.org/10.3390/app14146214
56. Yazici, İ, Shayea, I., & Din, J. (2023). A survey of applications of artificial intelligence and machine learning in future mobile networks-enabled systems. *Engineering Science Technology an International Journal, 44*, 101455. https://doi.org/10.1016/j.jestch.2023.101455
57. Alzubaidi, L., Bai, J., Al-Sabaawi, A., et al. (2023). A survey on deep learning tools dealing with data scarcity: Definitions, challenges, solutions, tips, and applications. *Journal Big Data, 10*, 46. https://doi.org/10.1186/s40537-023-00727-2

Arif Karadag was born in 1982. He received the Ph.D. degree from Sakarya University. He is currently working an assistant professor in motor vehicles and transportation technologies depermetn at Mus Alparslan University. His current research interests include welding, composite coatings, additive manufacturing, mechanical tests and composite polymers.

Osman Ulkir was born in 1990. He received the Ph.D. degree from Marmara University. He is currently working an assistant professor in electric and energy depermetn at Mus Alparslan University. His current research interests include mechatronics system design, additive manufacturing, artificial intelligent, biomechatronics, and composite polymers.